PNAS
www.pnas.org

Supplementary Information for

The environmental limits of Rift Valley Fever revealed using eco-epidemiological mechanistic models

Giovanni Lo Iacono, Andrew A. Cunningham, Bernard Bett, Delia Grace, David W. Redding, James L. N. Wood

Giovanni Lo Iacono.
E-mail: g.loiacono@surrey.ac.uk

This PDF file includes:

Supplementary text
Figs. S1 to S29
Tables S1 to S7
References for SI reference citations

Supporting Information Text

Full details of mathematical models.

Empirical patterns in temperature and water bodies for Kenya

We used empirical temperatures and water bodies data for Kenya. Daily temperature data, from 01−Jan−2000 to 21−Dec−2013, were downloaded from the Global Historical Climatology Network (1) based on a network of 5 stations (displayed in Fig. S1) located in Lodwar (latitude: 3° 7′ 1.2″ N, longitude 35° 37′ 1.2″ E), Garissa (0° 28′ 1.2″ S, 39° 37′ 58.8″ E), Jomo Kenyatta International airport (1° 19′ 1.2″ S, 36° 55′ 1.2″ E), Mandera (3° 55′ 58.8″ N, 41° 52′ 1.2″ E), and Mombasa (4° 1′ 58.8″ S, 39° 37′ 1.2″ E). Here, the daily temperature data were spatially averaged leading to the time series of temperature shown in Fig. S2 and Fig. S3.

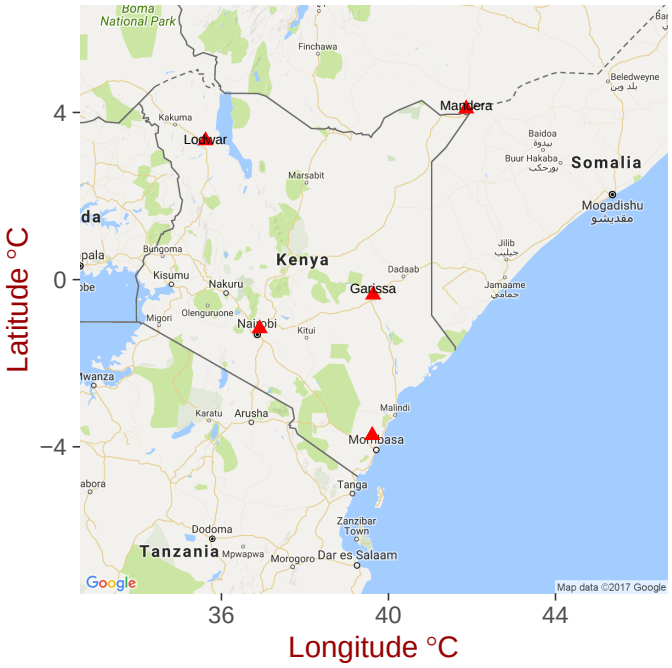

Fig. S1. Meteorological stations, represented by red triangles, where temperature data were recorded (1).

Satellite data of permanent and seasonal water bodies, natural and man-made, from 01−Jan−2000 to 21−Dec−2013, were downloaded from Copernicus Global Land Service (2). The satellite data were downloaded as GeoTIFF files (a metadata standard allowing geo-referencing information to be embedded within a TIFF file). Each file corresponds to a square image (tile) covering an area of $10° \times 10°$. The entire territory of Kenya is covered by four square tiles, which were combined together and then intersected with ESRI shapefile representing the border of Kenya. Each pixel of the GeoTIFF file is associated with a digital code identify the type of land cover such as fresh water or dry land (see (2) and in particular (3).

The angular pixel resolution (1/112 degree) was converted into metric pixel resolution as $\pi R_{Earth}(1/112)/180 = 993\ m$ where $R_{Earth} = 6378\ 10^3\ m$ is the terrestrial radius at the equator. Thus the satellite detects surfaces covered by water with a size of about 1 km^2 (2). The data are provided for the three dekads of every month of the year (first dekad of the month goes from day 1 to day 10, second dekad from day 11 to day 20 and third dekad from day 21 to the end of the month). Finally we identified all the pixels labelled as "fresh water" and calculate, for each dekads, the total surface of water bodies for the entire country. The satellite data were processed by using R package 'Raster' (4). Here, we used the total water bodies surface from Kenya rescaled by the factor $\mathcal{A}/S_{Kenya}$, where S_{Kenya} is the area of Kenya and $\mathcal{A} = 1E6\ m^2$ is the typical area that we assume to be scanned by *Aedes* sp. and *Culex* sp. fliers. This leads to the time series of water bodies shown in Fig. S4 and S5.

It might be instructive to relate the theoretical case, (*i.e.* simple sinusoidal variation of the surface area of water bodies and of temperature) with the realistic situation. For indicative purposes only, therefore we used wavelet analysis (Figs. S6 and S7 for temperature and S8 and S9 for water bodies) to explore and compare the periodicity of temperatures and water bodies surfaces. The analysis showed that for temperature the dominant period is 1 year with contributions of the second (6 months) and third (4 months) harmonics. In contrast, water bodies dynamics is dominated by the second harmonic, corresponding to 6 months. Thus realistic temperature and water bodies could be approximated by simple periodic functions with 1 year and 6 month period respectively. The statistical significance of the patterns exhibited by the wavelet approach was assessed using bootstrapping methods. The idea is to construct, from observed time series, control data sets, which share some properties with the original series but are constructed under a defined null hypothesis, *i.e. the variability of the observed time-series or the association between two time-series is no different to that expected from a purely random process* (5). The level of wavelet

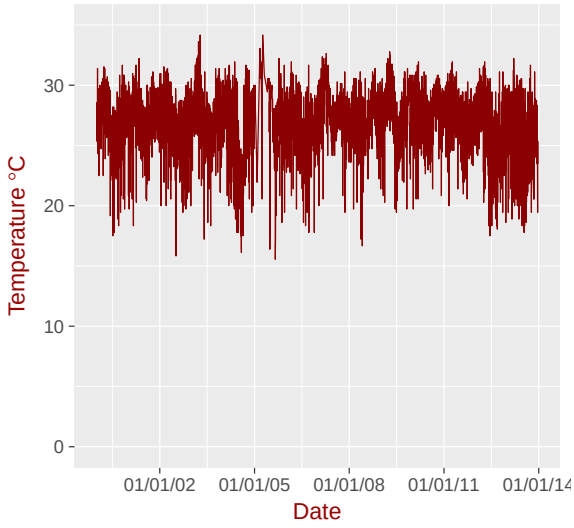

Fig. S2. Time-series of daily temperatures averaged over the five stations shown in Fig. S1.

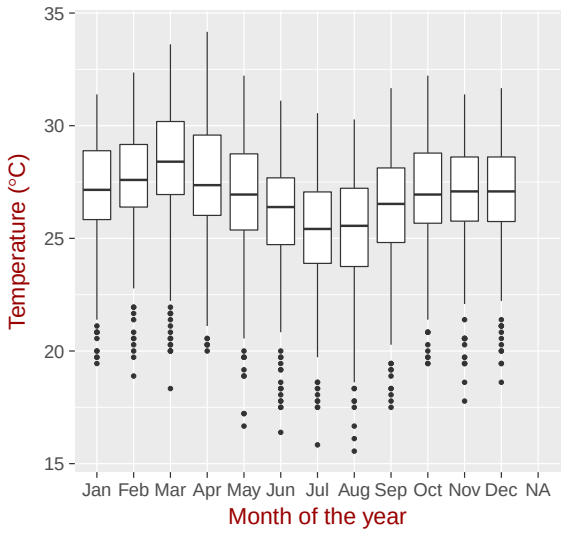

Fig. S3. Boxplot of temperatures from the time series in Fig. S2 showing summary statistics, minimum, first quartile, median, third quartile, and maximum and outliers, of temperature for each month.

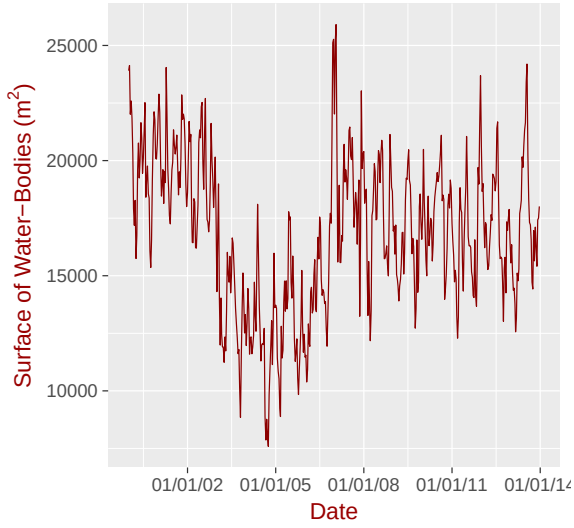

Fig. S4. Time-series of of total water bodies surface from Kenya from satellite images rescaled by the factor $\mathcal{A}/S_{Kenya}$ (2).

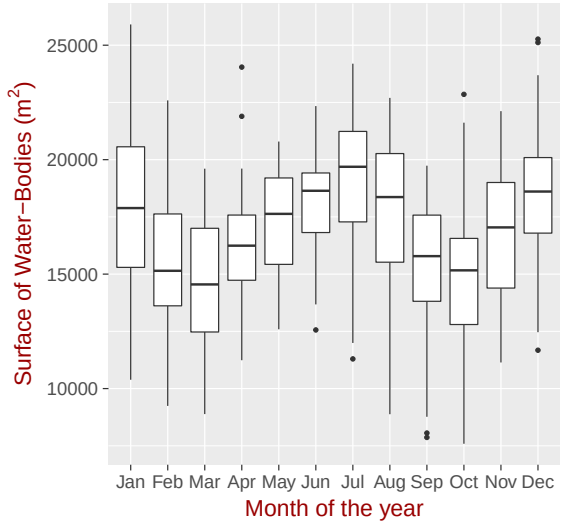

Fig. S5. Boxplot of total water bodies surface from Fig. S4 showing summary statistics, minimum, first quartile, median, third quartile, and maximum and outliers, of water bodies surface for each month.

power significance applied for inclusion of reconstruction waves was 0.05. The computed significant levels were based on 100 bootstrapped series (Rosch A, Schmidbauer H (2014) WaveletComp: A guided tour through the R-package).

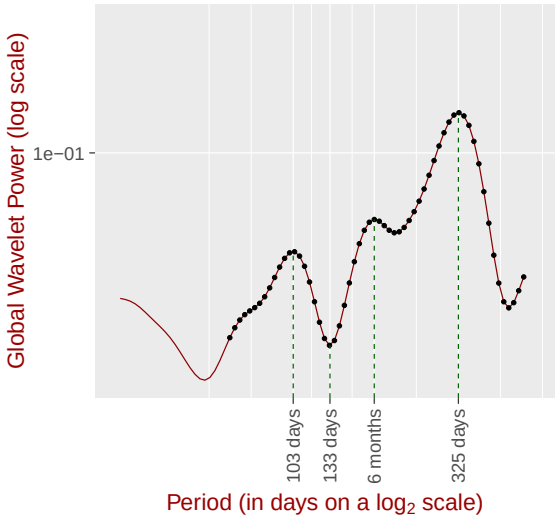

Fig. S6. Global average wavelet power spectrum of the root transformed time-series of temperature.

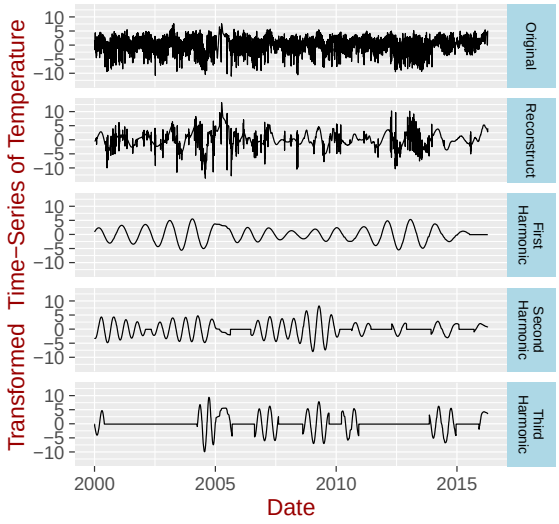

Fig. S7. Original and reconstructed time-series according to all harmonics and the selected first 3 harmonics only (bottom).

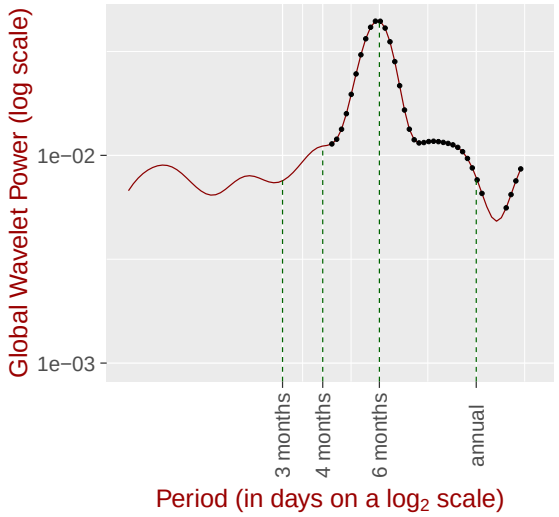

Fig. S8. Global average wavelet power spectrum of the root transformed time-series of total water bodies surface.

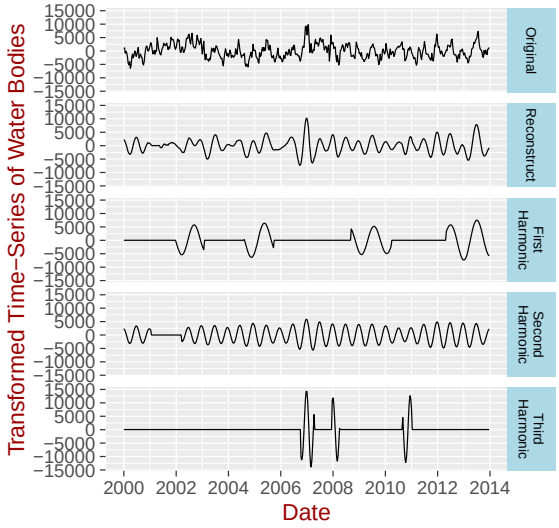

Fig. S9. Original and reconstructed time-series according to all harmonics and the selected first 3 harmonics only.

Population model for mosquito population and RVFV

First, we introduce the ecological model for the mosquito population (*Culex* sp. and *Aedes* sp.) in absence of RVFV, then we extend the model to include the dynamics of RVFV in the populations of mosquito and livestock.

Ecological model for mosquito population in absence of RVFV. The model is largely based on the stage-structured, population dynamics model of Otero *et al.* (6), which includes the effect of temperature on the development rate of the mosquitoes. Important additions to Otero *et al.*'s model are: i) the dependence of the oviposition process on the availability of water bodies ii) the separation of *Aedes* sp. eggs in mature and immature eggs; iii) the dependency of the number of eggs per batch on the density of livestock. As the oviposition process is different for *Aedes* sp. and *Culex* sp., the respective population models are different.

***Culex* mosquito population model. No disease.** The population of mosquitoes is divided into six different mosquito stages: eggs O_C, larvae L_C, pupae P_C, nulliparous female, *i.e.* female adults not having laid eggs C_1, flyers F_C, and female adults having laid

eggs C_2. Adult male mosquitoes are not explicitly included, and only one half of the emerging adults are females (therefore the factor 1/2 in the 4^{th} equation in the system 1). Once the gonotrophic cycle $\tilde{\theta}_{C1}^{\text{Culex}}$ ends, the nulliparous female begins to fly, becoming a flyer F_C in search of breeding sites followed by a series of cyclic transitions, regulated by the gonotrophic cycle $\tilde{\theta}_{C2}^{\text{Culex}}$, to the adult stage C_2 and back to the flyer status F_C. A schematic of the model is presented in figure S10, the state variables and parameters are listed in table S2 and table S3 respectively. The population dynamics is then described by the following set of differential equations:

$$\begin{aligned}
\frac{\mathrm{d}O_C}{\mathrm{d}t} &= \xi^{\text{Culex}} F_C - \mu_O^{\text{Culex}} O_C - \theta_O^{\text{Culex}} O_C \\
\frac{\mathrm{d}L_C}{\mathrm{d}t} &= \theta_O^{\text{Culex}} O_C - \mu_L^{\text{Culex}} L_C - \theta_L^{\text{Culex}} L_C \\
\frac{\mathrm{d}P_C}{\mathrm{d}t} &= \theta_L^{\text{Culex}} L_C - \mu_P^{\text{Culex}} P_C - \theta_P^{\text{Culex}} P_C \\
\frac{\mathrm{d}C_1}{\mathrm{d}t} &= \frac{1}{2}\theta_P^{\text{Culex}}(\delta_E^{\text{Culex}}) P_C - \mu^{\text{Culex}} C_1 - \tilde{\theta}_{C1}^{\text{Culex}} C_1 \\
\frac{\mathrm{d}F_C}{\mathrm{d}t} &= \tilde{\theta}_{C1}^{\text{Culex}} C_1 + \tilde{\theta}_{C2}^{\text{Culex}} C_2 - \eta^{\text{Culex}} F_C - \mu^{\text{Culex}} F_C \\
\frac{\mathrm{d}C_2}{\mathrm{d}t} &= \eta^{\text{Culex}} F_C - \mu^{\text{Culex}} C_2 - \tilde{\theta}_{C2}^{\text{Culex}} C_2
\end{aligned} \qquad [1]$$

where ξ^{Culex} is a density dependent egg load rate (*i.e.* number of eggs laid by a flyer per time unit), η^{Culex} is the oviposition rate (*i.e.* number of times a flyer lay a batch of eggs per time unit), μ_O^{Culex}, μ_L^{Culex}, μ_P^{Culex}, and μ^{Culex} are the mortality rates for eggs, larvae, pupae and adults *Culex* sp., θ_O^{Culex}, θ_L^{Culex} and θ_P^{Culex} are the development rates for eggs, larvae and pupae, the rates to complete the first and second gonotrophic cycles, $\tilde{\theta}_{C1}^{\text{Culex}}$ and $\tilde{\theta}_{C2}^{\text{Culex}}$, are assumed to be the same are the biting rates (which differ for for the two adult stages). The symbol ˜ indicate that the gonotrophic cycle depends on the density of the livestock and it is discussed below.

Besides the daily mortality in the pupal stage, there is an additional mortality δ_E^{Culex} associated with the emergence of the adult. These parameters in general depend on temperature, availability of breeding sites (water bodies) and density of livestock and are discussed in details in the sections below.

***Aedes* mosquito population model. No disease.** The model for *Aedes* sp. has a similar, but not identical, structure of the the one for *Culex* sp.; key differences are i) *Aedes* sp. female lay their eggs in the moist soils above the water surrounding the water body and not on the water surface (Fig. S14) and ii) the eggs need to be submerged with water, after a minimum desiccation period to hatch, they are resistant to desiccation and can survive for periods of many years. Therefore, the model needs to differentiate among immature, O_I, and mature eggs O_M, as well as larvae L_A, pupae P_A, nulliparous female, A_1, flyers F_A, and female adults having laid eggs A_2. Newly laid eggs O_I need a minimum time (the minimum desiccation period) to develop to a mature stage O_M and then they stay in the mature stage until they are submerged with water. Adult male mosquitoes are not explicitly included, and only one half of the emerging adults are females (therefore the factor 1/2 in the 5^{th} equation in the system 2). Once the gonotrophic cycle $\tilde{\theta}_{A1}^{\text{Aedes}}$ ends, the nulliparous female begins to fly, becoming a flyer F_A in search of breeding sites followed by a series of cyclic transitions, regulated by the gonotrophic cycle $\tilde{\theta}_{A2}^{\text{Aedes}}$, to the adult stage A_2 and back to the flyer status F_A. A schematic of the model is presented in figure S11, the state variables and parameters are listed in table S2 and table S4 respectively. The population dynamics is then described by the following set of differential equations:

$$\begin{aligned}
\frac{\mathrm{d}O_I}{\mathrm{d}t} &= \xi^{\text{Aedes}} F_A - \mu_{Oi}^{\text{Aedes}} O_I - \theta_{Oi}^{\text{Aedes}} O_I \\
\frac{\mathrm{d}O_M}{\mathrm{d}t} &= (1-\delta_{sp})\theta_{Oi}^{\text{Aedes}} O_I - \mu_{Om}^{\text{Aedes}} O_M - \tau_O^{\text{Aedes}} O_M \\
\frac{\mathrm{d}L_A}{\mathrm{d}t} &= \tau_O^{\text{Aedes}} O_M - \mu_L^{\text{Aedes}} L_A - \theta_L^{\text{Aedes}} L_A + \delta_{sp}\theta_{Oi}^{\text{Aedes}} O_I \\
\frac{\mathrm{d}P_A}{\mathrm{d}t} &= \theta_L^{\text{Aedes}} L_A - \mu_P^{\text{Aedes}} P_A - \theta_P^{\text{Aedes}} P_A \\
\frac{\mathrm{d}A_1}{\mathrm{d}t} &= \frac{1}{2}\theta_P^{\text{Aedes}}(\delta_E^{\text{Aedes}}) P_A - \mu^{\text{Aedes}} A_1 - \tilde{\theta}_{A1}^{\text{Aedes}} A_1 \\
\frac{\mathrm{d}F_A}{\mathrm{d}t} &= \tilde{\theta}_{A1}^{\text{Aedes}} A_1 + \tilde{\theta}_{A2}^{\text{Aedes}} A_2 - \eta^{\text{Aedes}} F_A - \mu^{\text{Aedes}} F_A \\
\frac{\mathrm{d}A_2}{\mathrm{d}t} &= \eta^{\text{Aedes}} F_A - \mu^{\text{Aedes}} A_2 - \tilde{\theta}_{A2}^{\text{Aedes}} A_2
\end{aligned} \qquad [2]$$

where, in analogy with the model for *Culex* sp., ξ^{Aedes} is a density dependent egg load rate, η^{Aedes} is the oviposition rate, μ_{Oi}^{Aedes}, μ_{Om}^{Aedes}, μ_L^{Aedes}, μ_P^{Aedes} and μ^{Aedes} are the mortality rates for immature eggs, mature eggs, larvae, pupae and adults; $\theta_{Oi}^{\text{Aedes}}$, θ_L^{Aedes} and θ_P^{Aedes} are the developmental rate for immature eggs, larvae and pupae for *Aedes* sp., the rates to complete

the first and second gonotrophic cycles, $\tilde{\theta}_{A1}^{\text{Aedes}}$ and $\tilde{\theta}_{A2}^{\text{Aedes}}$, are assumed to be the same are the biting rates (which differ for for the two adult stages). The symbol ˜ indicate that the gonotrophic cycle depends on the density of the livestock and it is discussed below. τ_O^{Aedes} is the developmental rate from mature eggs to larvae, where we used a different notation from the other developmental rates to emphasize that the rate depends on the water bodies surface and not on the temperature. Besides the daily mortality in the pupal stage, there is an additional mortality δ_E^{Aedes} associated with the emergence of the adult. The term $\delta_{sp} = 0.197$ (absent in the model for *Culex* sp.) takes into account the fact that 19.7% of newly embryonated eggs hatch spontaneously without flooding (7). These parameters in general depend on temperature, surface of water bodies and density of livestock, and are discussed in details in the sections below.

Impact of temperature, water bodies and density of livestock on the ecological parameters.

Oviposition rates η^{Culex} and η^{Aedes} and their dependency on the surface of water bodies.
According to (8), the average time for egg deposition is $t_{dep} = 0.229$ days in laboratory conditions, which are assumed to be ideal conditions. At field scale the flyers mosquitoes need to search for a suitable breeding site, reducing the oviposition rate. Let's assume that the typical surfaces scanned by adult flyers, either *Culex* sp. or *Aedes* spp, searching for a breeding site is $\mathcal{A}$, then a simple guess-estimate of the oviposition rates are:

$$\eta^{\text{Culex}} = \eta^{\text{Aedes}} \approx \frac{\sum_P S^P(t)}{\mathcal{A}} \frac{1}{t_{dep}} \quad [3]$$

where $S^P(t)$ is the surface of the pond P at time t. The searching area is estimated as $\mathcal{A} \approx 1E6 - 2E6m^2$ based on some indication that the spatial range of the activity of mosquitoes would be up to $1,500m$ to the nearest ponds(9).
Egg load rates ξ^{Culex} and ξ^{Aedes} and their dependency on the availability of breeding sites and density of livestock.
The egg load is expected to depend on the availability and suitability of breeding sites at time t, (*i.e.* the surface area of water bodies within the dispersal region of flyers) and the number of eggs already laid which reduces the available surface of water bodies. Thus, for *Culex* sp. the egg load rate ξ^{Culex} is modelled as:

$$\xi^{\text{Culex}} = \tilde{b}_C \eta^{\text{Culex}} \left(1 - \frac{O_C}{K_C}\right) \quad [4]$$

$\tilde{b}_C$ is the typical number of eggs per batch for *Culex* sp., O_C is the number of eggs already laid (which occupy part of the surface of water bodies), the carrying capacity K_C takes into account that the maximum number of eggs that can be laid over a water body is limited by its surface, $S^P(t)$:

$$K_C \approx \sum_P \rho_C \kappa^{\text{Culex}} S^P(t) \quad [5]$$

where ρ_C is the density of eggs per surface unit and $\kappa^{\text{Culex}} S^P(t)$ is the suitable breeding site, *i.e.* the inner area of the water body where *Culex* sp. lay their eggs (fig. S14). Here we assumed that the extent of this inner area is proportional to the size of the water body by a factor κ^{Culex}.

In addition, mosquitoes cannot produce eggs without ingesting blood meals, thus following the same argument presented in (10) for triatomines, the number of eggs per batch is assumed to be a decreasing function of the vector-to-host ratio *Culex* sp. m_C. Accordingly, the number of eggs per batch is modelled as:

$$\tilde{b}_C = \frac{b_C}{(1 + m_C/q)} \quad [6]$$

where b_C is the typical number of eggs produced per batch in the limit of infinite resources, q the particular vector-to-host ratio for which vector fecundity is divided by two. Accordingly, in absence of host ($m_C \to \infty$), *i.e.* no blood-meal, the number of eggs per batch drops to zero; conversely, in the limit of infinite resources (*i.e.* large number of host per mosquitoes, $m_C = 0$), the number of eggs per batch reaches its maximum. The vector-to-host ratio is calculated from the model as

$$m_C = p_f \frac{C_1 + C_2}{N_L} \quad [7]$$

as only adults female C_1 and C_2 are biting, N_L is the number of livestock, which, unless otherwise stated, it is assumed to be $N_L = 500$. The factor $p_f = 0.01$ takes into account that only a proportion (here assumed to be 1%) of the entire mosquito population will be able to detect and feed on the particular host species under consideration (the rest of the mosquitoes either feed on different species or die due to other causes such as predation).

The same arguments can be repeated for modeling the egg load rate for *Aedes* sp., leading to

$$\xi^{\text{Aedes}} = \tilde{b}_A \eta^{\text{Aedes}} \left(1 - \frac{O_I + O_M}{K_A}\right) \quad [8]$$

$\tilde{b}_A$ is the typical number of eggs per batch for *Aedes* sp., $O_I + O_M$ is the number of immature and mature eggs already laid, and the carrying capacity K_A is given by:

$$K_A \approx \sum_P \rho_A \kappa^{\text{Aedes}} S^P(t) \quad [9]$$

where ρ_A is the density of eggs per surface unit, this time the suitable breeding site, $\kappa^{\text{Aedes}} S^P(t)$, is represented by moist soil surrounding the water body where *Aedes* sp. lay their eggs (fig. S14). Here we assumed that this suitable area is proportional to the size of the water body by a factor κ^{Aedes}. The number of eggs per batch is modeled as:

$$\tilde{b}_A = \frac{b_A}{(1 + m_A/q)} \quad [10]$$

where b_A is the number of eggs produced per batch in the limit of infinite resources, m_A is the vector-to-host ratio for *Aedes* sp., and, as above, q is the particular vector-to-host ratio for which vector fecundity is divided by two. The vector-to-host ratio is calculated from the model as

$$m_A = p_f \frac{A_1 + A_2}{N_L} \quad [11]$$

as only adults female A_1 and A_2 are biting and N_L is the number of livestock. As for the *Culex* sp. case, the factor $p_f = 0.01$ takes into account that only a proportion of the entire mosquito population will be able to detect and feed on the particular host species under consideration.

Development rates and their dependency on temperature and water body surface.

The development rates are dependent on temperature. For *Culex* sp. there are five developmental rates in the model that correspond to egg hatching (θ_O^{Culex}), larval development (θ_L^{Culex}), pupal development (θ_P^{Culex}), first gonotrophic cycles ($\tilde{\theta}_{C1}^{\text{Culex}}$), and following gonotrophic cycles ($\tilde{\theta}_{C2}^{\text{Culex}}$). The developmental rates for the first gonotrophic cycle, assuming infinite availability of blood meal resources (*i.e.* large number of livestock), was modeled as (see (11) and references therein):

$$\theta_{C1}^{\text{Culex}} = 0.0173[(T - 273.15) - 9.6) \quad [12]$$

where the temperature was measured in Kelvin (K), while the developmental rate for the subsequent gonotrophic cycles was assumed to be twice the developmental rate for the first gonotrophic cycle ($\theta_{C2}^{\text{Culex}} = 2\theta_{C1}^{\text{Culex}}$ (based on (12)). This is based on the argument that the largest proportion of the gonotrophic cycle consists of maturation of the eggs which is temperature dependent. As done for the numbers of eggs per batch, we applied the correction proposed by (10), to the biting rates, *i.e.* the number of gonotrophic cycles per time unit. Accordingly:

$$\begin{aligned} \tilde{\theta}_{C1}^{\text{Culex}} &= \frac{\theta_{C1}^{\text{Culex}}}{(1 + m_C/q)} \\ \tilde{\theta}_{C2}^{\text{Culex}} &= \frac{\theta_{C2}^{\text{Culex}}}{(1 + m_C/q)} \end{aligned} \quad [13]$$

The development rates for the remaining stages were modeled according to the Schoolfield simplification of the Sharpe and DeMichele model for poikilotherm development (13). According to this model the maturation process is controlled by one enzyme which is active in a given temperature range and is deactivated only at high temperatures. In general terms, the mean development rate $\theta_x^{\text{Aedes}}(T)$ takes the form:

$$\theta_x^{\text{Culex}}(T) = \theta_x^{\text{Culex}}(298K) \frac{(T/298) \exp(\Delta H_A/R)(1/298 - 1/T)}{1 + \exp(\Delta H_H/R)(1/T_{1/2} - 1/T)} \quad [14]$$

$\theta_x^{\text{Culex}}(298K)$ is the development rate at $298K$ ($25°C$) assuming no enzyme inactivation, ΔH_A and ΔH_H are changes in the thermodynamics enthalpies characteristic of the organism, R is the universal gas constant, and $T_{1/2}$ is the temperature when half of the enzyme is deactivated because of high temperature. As we had no data, we assumed that the duration to complete egg hatching is half of the duration from egg hatch to first instar (*i.e.* when the larva moult for the first times out of four times before pupation). The particular values of the parameters in equation Eq. (14) are listed in table S6, can be found in (6, 14) and they are displayed in Fig. S15.

For *Aedes* sp. there are six developmental rates in the model that correspond to egg maturation ($\theta_{OI}^{\text{Aedes}}$), egg hatching ($\tau_O^{\text{Aedes}}$), larval development ($\theta_L^{\text{Aedes}}$), pupal development ($\theta_P^{\text{Aedes}}$), first gonotrophic cycles ($\tilde{\theta}_{A1}^{\text{Aedes}}$), and following gonotrophic cycles ($\tilde{\theta}_{A2}^{\text{Aedes}}$).

The number of hatching eggs from a pool of eggs laid by *Aedes* sp. at time $t - k$, will be null if k is less than the minimum desiccation period T_d or if the eggs were submerged in water before achieving the minimum desiccation period. Therefore the development time newly laid eggs O_I must satisfy two conditions, *i.e.*

$$\frac{1}{\theta_{OI}^{\text{Aedes}}} \approx \max\left(T_d, \frac{1}{\theta_O^{\text{Aedes}}[T(t)]}\right) \quad [15]$$

where $\theta_O^{\text{Aedes}}[T(t)]$ is the temperature dependency of development rate of the eggs calculated according to the Schoolfield simplification of the Sharpe and DeMichele model for poikilotherm development (13) (equation 21 below). Equation Eq. (15) is based on the assumption that dessication and temperature act independently on the physiology regulating the development rate of the eggs.

Eggs will hatch at the time of the first flood (*e.g.* at time t when $S^P(t) - S^P(t-\Delta t) > 0$) occurring since they entered the mature stage. For simplicity let's consider only one water body P, and we ignore the birth and death terms, during the small time Δt the variation in the number of mature eggs is given by:

$$O_M(t) - O_M(t-\Delta t) \approx -\overbrace{\max\left[\rho_A(t)\left(\kappa^{\text{Aedes}} S^P(t) - \kappa^{\text{Aedes}} S^P(t-\Delta t)\right), 0\right]}^{\text{Number of submerged eggs}} \quad [16]$$

i.e. if the water body is shrinking, no eggs will be submerged and no egg will hatch; the term $\kappa^{\text{Aedes}} S^P(t)$ is the breeding site (the brown area in figure S14, representing moist soil around the pond suitable for laying eggs) were we assumed that this area is proportional to the size of the pond by a factor κ^{Aedes}, $\rho_A(t)$ is the density of eggs (number of eggs per area) at time t, it can be estimated as

$$\rho_A(t) = \frac{O_I(t) + O_M(t)}{\kappa^{\text{Aedes}} S^P(t)} \approx \frac{O_M(t)}{\kappa^{\text{Aedes}} S^P(t)} \quad [17]$$

where, as previously done, $\kappa^{\text{Aedes}} S^P(t)$ is an estimation of the area of suitable breeding sites. Thus:

$$O_M(t) - O_M(t-\Delta t) = -\max\left[\frac{\left(S^P(t) - S^P(t-\Delta t)\right)}{S^P(t)}, 0\right] O_M(t) \quad [18]$$

The continuous counterpart of the above equation leads to:

$$\tau_O^{\text{Aedes}} = \max\left(\frac{1}{S^P(t)}\frac{\mathrm{d}S^P(t)}{\mathrm{d}t}, 0\right) \quad [19]$$

The term $\frac{\mathrm{d}S^P(t)}{\mathrm{d}t}$ represents the rate of change of the surface of the water bodies.

The developmental rates for the gonotrophic cycle were assumed to have the same functional form as for *Culex* sp., (see (11) and references therein):

$$\begin{aligned}
\tilde{\theta}_{A1}^{\text{Aedes}} &= \frac{\theta_{A1}^{\text{Aedes}}}{(1 + m_A/q)} \\
\tilde{\theta}_{A2}^{\text{Aedes}} &= \frac{\theta_{A2}^{\text{Aedes}}}{(1 + m_A/q)} \\
\theta^{\text{Aedes}}{}_{A1} &= 0.0173[(T - 273.15) - 9.6)] \\
\theta_{A2}^{\text{Aedes}} &= 2\theta_{A1}^{\text{Aedes}}
\end{aligned} \quad [20]$$

where the temperature was measured in Kelvin K. The development rates for the remaining stages were modelled according to the Schoolfield simplification of the Sharpe and DeMichele model for poikilotherm development (13):

$$\theta_x^{\text{Aedes}}(T) = \theta_x^{\text{Aedes}}(298^\circ K)\frac{(T/298)\exp\left(\Delta H_A/R\right)(1/298 - 1/T)}{1 + \exp\left(\Delta H_H/R\right)(1/T_{1/2} - 1/T)} \quad [21]$$

where the symbols have, *mutatis mutandis* the same meaning as in equation 14 for *Culex* sp. The particular values of the parameters in equation Eq. (21) are listed in table S6 and Fig. S16.

Mortality rates and their dependency on temperature. Mortality rates, and their dependency on temperature, for the specific stages were obtained from the literature (see table S3 and S4). When this was not possible as in the case for mortality associated with larvae and pupae, lifestage-specific mortality rates for *Culex quinquefasciatus* and *Aedes aegypti* were extracted from data collected under standard laboratory conditions by Rueda *et al.* (14). In particular, we assumed an exponential decay of the population of mosquitoes for each stage (as there is no mosquito births of in the experiment of (14)), leading to:

$$\begin{aligned}
N_L^{\text{Culex}}(t) &= N_L^{\text{Culex}}(t_0)\exp\left[-\mu_L^{\text{Culex}}(t - t_0)\right] \\
N_P^{\text{Culex}}(t) &= N_P^{\text{Aedes}}(t_0)\exp\left[-\mu_P^{\text{Culex}}(t - t_0)\right] \\
N_L^{\text{Aedes}}(t) &= N_L^{\text{Aedes}}(t_0)\exp\left[-\mu_L^{\text{Aedes}}(t - t_0)\right] \\
N_P^{\text{Aedes}}(t) &= N_P^{\text{Aedes}}(t_0)\exp\left[-\mu_P^{\text{Aedes}}(t - t_0)\right]
\end{aligned} \quad [22]$$

where $N_L^{\text{Culex}}(t)$ and $N_P^{\text{Culex}}(t)$ are respectively the numbers of larvae and pupae at time t for *Culex* sp.; similarly, $N_P^{\text{Aedes}}(t)$ and $N_P^{\text{Aedes}}(t)$ are respectively the numbers of larvae and pupae at time t for *Aedes* sp.; t_0 is the initial time set as reference; μ_L^{Culex} and μ_P^{Culex} are the mortality rates for larvae and pupae for *Culex* sp.; similarly, μ_L^{Aedes} and μ_P^{Aedes} are the mortality rates for larvae and pupae for *Aedes* sp. Values of N_L^{Culex} and N_L^{Aedes} at the particular time points were also estimated from the experiment of (14). More precisely, Rueda *et al.* (14) provided information (tables 1 and 2 in (14) and reproduced here in Tab S7)) to estimate the mean number of days for development of *Culex quinquefasciatus* and *Aedes aegypti* from egg hatch (set at time $t = 0$ in each experiment) to larva, denoted respectively t_L^{Culex} and t_L^{Aedes}, and from larva to pupa, denoted respectively t_P^{Culex} and t_P^{Aedes}, at six constant temperatures, T, ($15°C$, $20°C$, $25°C$, $27°C$, $30°C$ and $34°C$). Furthermore, Rueda *et al.* (14) (table 6 and reproduced here in Tab S7) provided the effect of constant temperatures on *Culex quinquefasciatus* and *Aedes aegypti* survival from egg hatch to adult stage. The authors also provided the proportion of total mortality, averaged over all temperatures, occurring during each stage. These were about 55% from eggs to larvae and 42% from larvae to pupae for *Culex quinquefasciatus* and about 98% from eggs to larvae and 2% from larvae to pupae for *Aedes aegypti*. Based on these information we estimated, for the six temperatures T, the ratios:

$$\begin{aligned}
\frac{N_L^{\text{Culex}}(t_L^{\text{Culex}})}{N_L^{\text{Culex}}(0)} &= 0.55(1 - S^{\text{Culex}}(T)) \\
\frac{N_L^{\text{Aedes}}(t_L^{\text{Aedes}})}{N_L^{\text{Aedes}}(0)} &= 0.98(1 - S^{\text{Aedes}}(T)) \\
\frac{N_P^{\text{Culex}}(t_P^{\text{Culex}})}{N_P^{\text{Culex}}(t_L^{\text{Culex}})} &= 0.42(1 - S^{\text{Culex}}(T)) \\
\frac{N_P^{\text{Aedes}}(t_P^{\text{Aedes}})}{N_P^{\text{Aedes}}(t_L^{\text{Aedes}})} &= 0.2(1 - S^{\text{Aedes}}(T))
\end{aligned} \qquad [23]$$

where $S^{\text{Culex}}(T)$ and $S^{\text{Culex}}(T)$ are the temperature dependent survival from egg hatch to adult stage for *Culex quinquefasciatus* and $S^{\text{Aedes}}(T)$ $S^{\text{Aedes}}(T)$ are the temperature dependent survival from egg hatch to adult stage for *Aedes aegypti* (Tab S7). From equations 22 , 23 and the mean number of days for development we estimated the mortality rates at different temperatures. Ordinary least squares regression models with quadratic terms, were fitted with mortality rate as the response variable and temperature ($15 - 34°C$) as the explanatory variable (Figs. S17-S18). The mortality curves for *Culex quinquefasciatus* and *Aedes aegypti* were considered representative of the mortality for *Culex* sp. and *Aedes* sp.

Extension of the above model to include the disease. We now link the ecological model for the population of *Culex* sp. and *Aedes* sp. developed above with the dynamics of RVFV in the populations of mosquitoes and livestock. We consider only one host, but the model can be readily extended to multiple heterogeneous hosts (*e.g.* goats, cattle, sheep). The model is described by a SEIR compartmental model for the livestock and stage-structured SEI model for the two mosquito populations. A scheme of the model is presented in figure S12. Both adult *Culex* sp. and *Aedes* sp. can become infected after feeding on infectious livestock I_L (thus movement out from the susceptible to the exposed category only happens during biting). More precisely, for *Culex* sp., the movement out from the susceptible categories, C_1 and C_2, are $\tilde{\theta}_{C1}^{Culex} C_1$ and $\tilde{\theta}_{C2}^{Culex} C_2$ respectively; out of these, $\lambda_{L\to C_1} C_1$ and $\lambda_{L\to C_2} C_2$ mosquitoes move to the exposed, flyer category, F_C^{Exp}. The remaining $(\tilde{\theta}_{C1}^{Culex} - \lambda_{L\to C_1})C_1$ and $(\tilde{\theta}_{C2}^{Culex} - \lambda_{L\to C_2})C_2$ move to the susceptible, flyer category, F_C (note that the terms $\lambda_{L\to C_1} C_1$ and $\lambda_{L\to C_2} C_2$ are smaller fractions of the terms $\tilde{\theta}_{C1}^{Culex}$ and $\tilde{\theta}_{C2}^{Culex}$, see equations Eq. (27)). The exposed categories then transit to the adult infectious categories C_1^{Inf} and C_2^{Inf} with rate ϵ_C. The identical argument can be repeated for *Aedes* sp., with the exception that there is an additional infectious category for nulliparous mosquitoes, A_1^{Inf}, emerging out of infectious eggs due to transovarial transmission. More precisely, all exposed and infectious adults, A_2^{Exp}, A_1^{Inf} and A_2^{Inf}, will deposit infectious eggs O_I^{Inf} (as there is no evidence of eggs in the exposed category) which will turn into infectious larva L_A^{Inf}, infectious pupae, P_A^{Inf}, and infectious adults, A_1^{Inf}, F_A^{Inf} and A_2^{Inf}. The model is described by the following set of differential equations:

Culex Susceptible Population

$$\begin{aligned}
\frac{\mathrm{d}O_C}{\mathrm{d}t} &= \zeta^{\text{Culex}}(F_C + (1-\alpha)(F_C^{\text{Inf}} + F_C^{\text{Exp}})) - \mu_O^{\text{Culex}} O_C - \theta_O^{\text{Culex}} O_C \\
\frac{\mathrm{d}L_C}{\mathrm{d}t} &= \theta_O^{\text{Culex}} O_C - \mu_L^{\text{Culex}} L_C - \theta_L^{\text{Culex}} L_C \\
\frac{\mathrm{d}P_C}{\mathrm{d}t} &= \theta_L^{\text{Culex}} L_C - \mu_P^{\text{Culex}} P_C - \theta_P^{\text{Culex}} P_C \\
\frac{\mathrm{d}C_1}{\mathrm{d}t} &= \theta_P^{\text{Culex}} (\delta_E^{\text{Culex}}/2) P_C - \mu^{\text{Culex}} C_1 - \tilde{\theta}_{C1}^{\text{Culex}} C_1 \\
\frac{\mathrm{d}F_C}{\mathrm{d}t} &= \left(\tilde{\theta}_{C1}^{\text{Culex}} - \lambda_{L\to C_1}\right) C_1 + \left(\tilde{\theta}_{C2}^{\text{Culex}} - \lambda_{L\to C_2}\right) C_2 - \eta^{\text{Culex}} F_C - \mu^{\text{Culex}} F_C \\
\frac{\mathrm{d}C_2}{\mathrm{d}t} &= \eta^{\text{Culex}} F_C - \mu^{\text{Culex}} C_2 - \tilde{\theta}_{C2}^{\text{Culex}} C_2
\end{aligned}$$

Culex Exposed Population

$$\begin{aligned}\frac{\mathrm{d}F_C^{\mathrm{Exp}}}{\mathrm{d}t} =&\tilde{\theta}_{C2}^{\mathrm{Culex}} C_2^{\mathrm{Exp}} - \eta^{\mathrm{Culex}} F_C^{\mathrm{Exp}} - \mu^{\mathrm{Culex}} F_C^{\mathrm{Exp}} - \epsilon_C F_C^{\mathrm{Exp}} + \lambda_{L\to C_1} C_1 + \lambda_{L\to C_2} C_2\\ \frac{\mathrm{d}C_2^{\mathrm{Exp}}}{\mathrm{d}t} =&-\mu^{\mathrm{Culex}} C_2^{\mathrm{Exp}} - \tilde{\theta}_{C2}^{\mathrm{Culex}} C_2^{\mathrm{Exp}} + \eta^{\mathrm{Culex}} F_C^{\mathrm{Exp}} - \epsilon_C C_2^{\mathrm{Exp}}\end{aligned}$$

Culex Infectious Population

$$\begin{aligned}\frac{\mathrm{d}F_C^{\mathrm{Inf}}}{\mathrm{d}t} =&\tilde{\theta}_{C2}^{\mathrm{Culex}} C_2^{\mathrm{Inf}} - \eta^{\mathrm{Culex}} F_C^{\mathrm{Inf}} - \mu^{\mathrm{Culex}} F_C^{\mathrm{Inf}} + \epsilon_C F_C^{\mathrm{Exp}}\\ \frac{\mathrm{d}C_2^{\mathrm{Inf}}}{\mathrm{d}t} =&-\mu^{\mathrm{Culex}} C_2^{\mathrm{Inf}} - \tilde{\theta}_{C2}^{\mathrm{Culex}} C_2^{\mathrm{Inf}} + \eta^{\mathrm{Culex}} F_C^{\mathrm{Inf}} + \epsilon_C C_2^{\mathrm{Exp}}\end{aligned}$$

Aedes Susceptible Population

$$\begin{aligned}\frac{\mathrm{d}O_I}{\mathrm{d}t} =&\zeta^{\mathrm{Aedes}}[F_A + (1-q_A)(F_A^{\mathrm{Inf}} + F_A^{\mathrm{Exp}})] - \mu_{Oi}^{\mathrm{Aedes}} O_I - \theta_{Oi}^{\mathrm{Aedes}} O_I\\ \frac{\mathrm{d}O_M}{\mathrm{d}t} =&(1-\delta_{sp})\theta_{Oi}^{\mathrm{Aedes}} O_I - \mu_{Om}^{\mathrm{Aedes}} O_M - \tau_O^{\mathrm{Aedes}} O_M\\ \frac{\mathrm{d}L_A}{\mathrm{d}t} =&\tau_O^{\mathrm{Aedes}} O_M - \mu_L^{\mathrm{Aedes}} L_A - \theta_L^{\mathrm{Aedes}} L_A + \delta_{sp}\theta_{Oi}^{\mathrm{Aedes}} O_I\\ \frac{\mathrm{d}P_A}{\mathrm{d}t} =&\theta_L^{\mathrm{Aedes}} L_A - \mu_P^{\mathrm{Aedes}} P_A - \theta_P^{\mathrm{Aedes}} P_A\\ \frac{\mathrm{d}A_1}{\mathrm{d}t} =&\theta_P^{\mathrm{Aedes}} (\delta_E^{\mathrm{Aedes}}/2) P_A - \mu^{\mathrm{Aedes}} A_1 - \tilde{\theta}_{A1}^{\mathrm{Aedes}} A_1\\ \frac{\mathrm{d}F_A}{\mathrm{d}t} =&\left(\tilde{\theta}_{A1}^{\mathrm{Aedes}} - \lambda_{L\to A_1}\right) A_1 + \left(\tilde{\theta}_{A2}^{\mathrm{Aedes}} - \lambda_{L\to A_2}\right) A_2 - \eta^{\mathrm{Aedes}} F_A - \mu^{\mathrm{Aedes}} F_A\\ \frac{\mathrm{d}A_2}{\mathrm{d}t} =&\eta^{\mathrm{Aedes}} F_A - \mu^{\mathrm{Aedes}} A_2 - \tilde{\theta}_{A2}^{\mathrm{Aedes}} A_2\end{aligned}$$

Aedes Exposed Population

$$\begin{aligned}\frac{\mathrm{d}F_A^{\mathrm{Exp}}}{\mathrm{d}t} =&\tilde{\theta}_{A2}^{\mathrm{Aedes}} A_2^{\mathrm{Exp}} - \eta^{\mathrm{Aedes}} F_A^{\mathrm{Exp}} - \mu^{\mathrm{Aedes}} F_A^{\mathrm{Exp}} - \epsilon_A F_A^{\mathrm{Exp}} + \lambda_{L\to A_1} A_1 + \lambda_{L\to A_2} A_2\\ \frac{\mathrm{d}A_2^{\mathrm{Exp}}}{\mathrm{d}t} =&-\epsilon_A A_2^{\mathrm{Exp}} - \mu^{\mathrm{Aedes}} A_2^{\mathrm{Exp}} - \tilde{\theta}_{A2}^{\mathrm{Aedes}} A_2^{\mathrm{Exp}} + \eta^{\mathrm{Aedes}} F_A^{\mathrm{Exp}}\end{aligned}$$

Aedes Infectious Population

$$\begin{aligned}\frac{\mathrm{d}O_I^{\mathrm{Inf}}}{\mathrm{d}t} =&\zeta^{\mathrm{Aedes}} q_A (F_A^{\mathrm{Inf}} + F_A^{\mathrm{Exp}}) - \mu_{Oi}^{\mathrm{Aedes}} O_I^{\mathrm{Inf}} - \theta_{Oi}^{\mathrm{Aedes}} O_I^{\mathrm{Inf}}\\ \frac{\mathrm{d}O_m^{\mathrm{Inf}}}{\mathrm{d}t} =&(1-\delta_{sp})\theta_{Oi}^{\mathrm{Aedes}} O_I^{\mathrm{Inf}} - \mu_{Om}^{\mathrm{Aedes}} O_m^{\mathrm{Inf}} - \tau_O^{\mathrm{Aedes}} O_m^{\mathrm{Inf}}\\ \frac{\mathrm{d}L_A^{\mathrm{Inf}}}{\mathrm{d}t} =&\tau_O^{\mathrm{Aedes}} O_m^{\mathrm{Inf}} - \mu_L^{\mathrm{Aedes}} L_A^{\mathrm{Inf}} - \theta_L^{\mathrm{Aedes}} L_A^{\mathrm{Inf}} + \delta_{sp}\theta_{Oi}^{\mathrm{Aedes}} O_I^{\mathrm{Inf}}\\ \frac{\mathrm{d}P_A^{\mathrm{Inf}}}{\mathrm{d}t} =&\theta_L^{\mathrm{Aedes}} L_A^{\mathrm{Inf}} - \mu_P^{\mathrm{Aedes}} P_A^{\mathrm{Inf}} - \theta_P^{\mathrm{Aedes}} P_A^{\mathrm{Inf}}\\ \frac{\mathrm{d}A_1^{\mathrm{Inf}}}{\mathrm{d}t} =&\theta_P^{\mathrm{Aedes}} (\delta_E^{\mathrm{Aedes}}/2) P_A^{\mathrm{Inf}} - \mu^{\mathrm{Aedes}} A_1^{\mathrm{Inf}} - \tilde{\theta}_{A1}^{\mathrm{Aedes}} A_1^{\mathrm{Inf}}\\ \frac{\mathrm{d}F_A^{\mathrm{Inf}}}{\mathrm{d}t} =&\tilde{\theta}_{A1}^{\mathrm{Aedes}} A_1^{\mathrm{Inf}} + \tilde{\theta}_{A2}^{\mathrm{Aedes}} A_2^{\mathrm{Inf}} - \eta^{\mathrm{Aedes}} F_A^{\mathrm{Inf}} - \mu^{\mathrm{Aedes}} F_A^{\mathrm{Inf}} + \epsilon_A F_A^{\mathrm{Exp}}\\ \frac{\mathrm{d}A_2^{\mathrm{Inf}}}{\mathrm{d}t} =&\eta^{\mathrm{Aedes}} F_A^{\mathrm{Inf}} - \mu^{\mathrm{Aedes}} A_2^{\mathrm{Inf}} - \tilde{\theta}_{A2}^{\mathrm{Aedes}} A_2^{\mathrm{Inf}} + \epsilon_A A_2^{\mathrm{Exp}}\end{aligned}$$

Livestock

$$\begin{aligned}\frac{\mathrm{d}S_L}{\mathrm{d}t} =& b_L N_L - \mu_L S_L - (\lambda_{A\to L} + \lambda_{C\to L})S_L \\ \frac{\mathrm{d}E_L}{\mathrm{d}t} =& (\lambda_{A\to L} + \lambda_{C\to L})S_L - \epsilon_L E_L - \mu_L E_L \\ \frac{\mathrm{d}I_L}{\mathrm{d}t} =& \epsilon_L E_L - \gamma_L I_L - \mu_L I_L \\ \frac{\mathrm{d}R_L}{\mathrm{d}t} =& \gamma_L I_L - \mu_L R_L\end{aligned} \quad [24]$$

where $\alpha = 0.21$ take into account that infected *Culex Pipiens* showed a 21% reduction in the feeding rate (15); $q_A = 0.007$ is the probability of transovarial transmission; ζ^{Culex} and ζ^{Aedes} are density dependent egg load rate, *i.e.* number of eggs laid by a flyer per time unit, similarly to ξ^{Culex}, ξ^{Aedes} previously introduced, these are defined as:

$$\begin{aligned}\zeta^{\text{Culex}} =& \frac{b_C}{(1 + (m_A^i + m_C)/q)} \eta^{\text{Culex}} \left(1 - \frac{O_C}{K_C}\right) \\ \zeta^{\text{Aedes}} =& \frac{b_A}{(1 + (m_A^i + m_C)/q)} \eta^{\text{Aedes}} \left(1 - \frac{O_I + O_M + O_I^{\text{Inf}} + O_m^{\text{Inf}}}{K_A}\right)\end{aligned} \quad [25]$$

where infected eggs have been included in the estimation. The vector-to-host ratios are estimated as:

$$\begin{aligned}m_C =& p_f \frac{C_1 + C_2 + C_2^{\text{Exp}} + C_2^{\text{Inf}}}{N_L} \\ m_A =& p_f \frac{A_1 + A_2 + A_2^{\text{Exp}} + A_1^{\text{Inf}} + A_2^{\text{Inf}}}{N_L} \\ N_L =& S_L + E_L + I_L + R_L\end{aligned} \quad [26]$$

The factor $p_f = 0.01$ takes into account that only a proportion (here assumed to be 1%) of the entire mosquito population will be able to detect and feed on the particular host species under consideration. The force of infections for *Culex* sp. and *Aedes* sp. are given by:

$$\begin{aligned}\lambda_{L\to C_1} =& \beta_{L\to C} \tilde{\theta}_{C1}^{\text{Culex}} \frac{I_L}{N_L} \\ \lambda_{L\to C_2} =& \beta_{L\to C} \tilde{\theta}_{C2}^{\text{Culex}} \frac{I_L}{N_L} \\ \lambda_{L\to A_1} =& \beta_{L\to A} \tilde{\theta}_{A1}^{\text{Aedes}} \frac{I_L}{N_L} \\ \lambda_{L\to A_2} =& \beta_{L\to A} \tilde{\theta}_{A2}^{\text{Aedes}} \frac{I_L}{N_L}\end{aligned} \quad [27]$$

where $\beta_{L\to C}$ and $\beta_{L\to A}$ are the probabilities of transmission from an infected livestock to *Culex* sp., and to *Aedes* sp. respectively, irrespective of the adult stage. S_L, E_L, I_L are the number of susceptible, exposed, infectious number of livestock, b_L is the birth rate of livestock, μ_L the natural mortality (we assumed no disease induced livestock mortality), ϵ_L and γ_L are the incubation and recover rates for livestock, $\lambda_{C\to L}$ and $\lambda_{A\to L}$ and are the force of infection from *Culex* sp. and *Aedes* sp. to livestock, given by:

$$\begin{aligned}\lambda_{C\to L} =& \left(\beta_{C\to L} m_C \frac{\tilde{\theta}_{C2}^{\text{Culex}} C_2^{\text{Inf}}}{C_1 + C_2 + C_2^{\text{Exp}} + C_2^{\text{Inf}}}\right) \\ \lambda_{A\to L} =& \left(\beta_{A\to L} m_A \frac{\tilde{\theta}_{A1}^{\text{Aedes}} A_1^{\text{Inf}} + \tilde{\theta}_{A2}^{\text{Aedes}} A_2^{\text{Inf}}}{A_1 + A_2 + A_2^{\text{Exp}} + A_1^{\text{Inf}} + A_2^{\text{Inf}}}\right)\end{aligned} \quad [28]$$

where $\beta_{C\to L}$ and $\beta_{A\to L}$ are the probability of transmission from an infected *Culex* sp. and infected *Aedes* sp. to livestock. The biting rates have been rescaled as:

$$\begin{aligned}\tilde{\theta}_{C1}^{\text{Culex}} &= \frac{\theta_{C1}^{\text{Culex}}}{(1+(m_A^i+m_C)/q)}\\ \tilde{\theta}_{C2}^{\text{Culex}} &= \frac{\theta_{C2}^{\text{Culex}}}{(1+(m_A^i+m_C)/q)}\\ \tilde{\theta}_{A1}^{\text{Aedes}} &= \frac{\theta_{A1}^{\text{Aedes}}}{(1+(m_A^i+m_C)/q)}\\ \tilde{\theta}_{A2}^{\text{Aedes}} &= \frac{\theta_{A2}^{\text{Aedes}}}{(1+(m_A^i+m_C)/q)}\end{aligned} \quad [29]$$

The extrinsic incubation period for *Culex* sp. and *Aedes* sp. depends on temperature and was modeled as (16)

$$\frac{1}{\epsilon_A} = \frac{1}{\epsilon_C} = [-0.1038 + 0.0071(T - 273.15)]^{-1} \quad [30]$$

where the temperature is expressed in Kelvin, K. All other parameters have been previously defined and presented in tables S3, S4, S5.

Inclusion of multiple hosts. Let consider the situation when we have multiple hosts for the feeding mosquitoes. Each host can be bitten by infected mosquitoes. Non-susceptible host will not get infected while other host get infected with different probabilities depending on the level of susceptibility of the host. Mosquitoes can be infected from the different types of infected hosts. Inclusion of multiple hosts result in a set of differential equations for the additional animals compartment, *i.e.* $S_L^{Host\ 1}$, $S_L^{Host\ 2}$, $E_L^{Host\ 1}$, $E_L^{Host\ 1}$, $I_L^{Host\ 1}$, $I_L^{Host\ 1}$, where the suffix $Host\ i$ refers to the $i-$host. As mosquitoes can be infected from the different types of infected hosts this results in extra terms in the differential equations for *Culex* sp. and *Aedes* sp. exposed categories. This extended model will require additional forces of infections from the particular host $Host\ i$ to *Culex* sp. and *Aedes* sp. and additional forces of infections from *Culex* sp. and *Aedes* sp. to the particular host $Host\ i$.

A key factor is that the biting rate is not the same for all host species. To take into account of the feeding preference, the biting rates ($\tilde{\theta}_{C1}^{\text{Culex}}$, $\tilde{\theta}_{C2}^{\text{Culex}}$, $\tilde{\theta}_{A1}^{\text{Aedes}}$, $\tilde{\theta}_{A2}^{\text{Aedes}}$) can be rescaled by the factor ψ_i, *i.e.* the proportion of bites on each host species given by:

$$\psi_i = \frac{\delta_i \left[S_L^{Host\ i} + E_L^{Host\ i} + I_L^{Host\ i} + R_L^{Host\ i}\right]}{\sum_j \delta_j \left[S_L^{Host\ j} + E_L^{Host\ j} + I_L^{Host\ j} + R_L^{Host\ j}\right]} \quad [31]$$

where δ_i is a measure of vector preference for host species i (17, 18). This has important consequences on the dynamics of the disease. For example, the presence of a non-susceptible host might result in a decrease of the infection prevalence if mosquitoes largely prefer to feed on it (dilution effect), but even a non-susceptible host might increase disease prevalence if its presence attract more mosquitoes and they prefer to feed on highly susceptible host. A more detailed discussion on this crucial topic is presented in (19). Unfortunately the vector feeding preference is rarely known and future fieldwork to measure this effect is sought after.

In both figures S10 and S11, blue lines indicate water bodies depending parameters, red lines indicate temperature depending parameters. The symbol * means that the rate at which the population leaves a particular category is different of the rate at which the same population enter a new category (for example *Culex* sp. flyers leave the adult flyers category with rate η^{Culex}, but they produce eggs entering the egg category with rate ξ^{Culex}). Apart using the same colors for the same categories, the choice of all other colors in figures S10, S11 and S12 is mainly for visual purpose only.

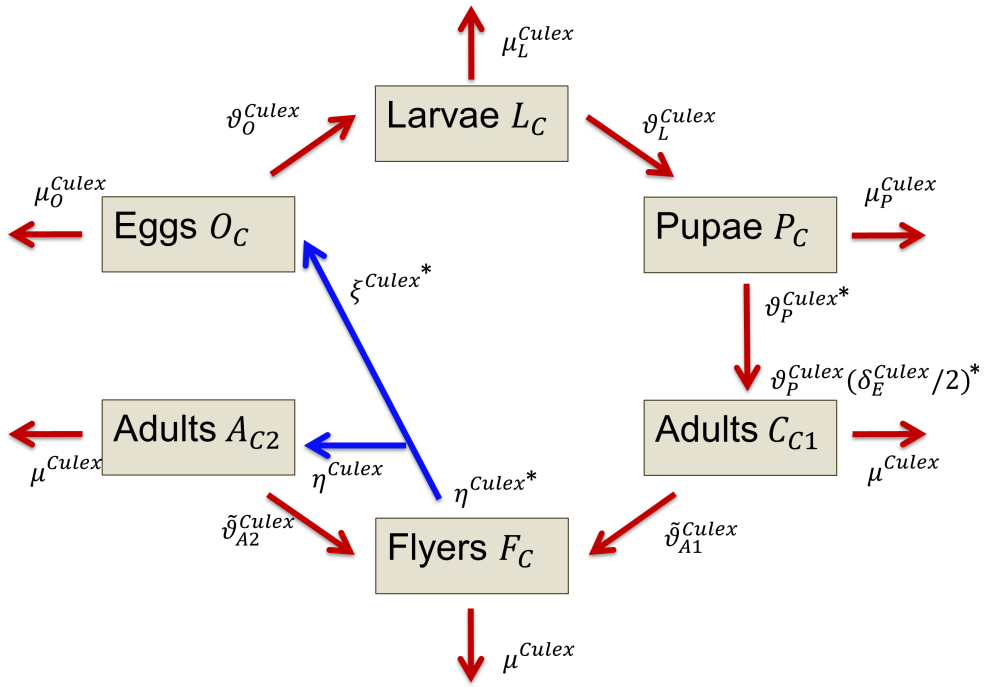

Fig. S10. Populations and events of the model for *Culex* sp. in absence of the disease.

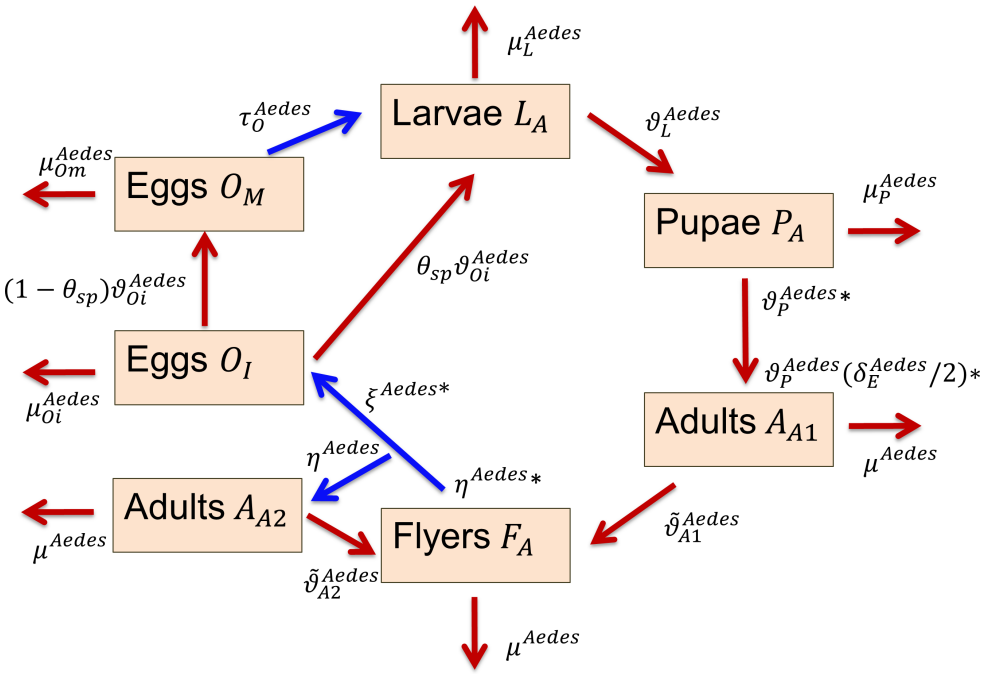

Fig. S11. Populations and events of the model for *Aedes* sp. in absence of the disease.

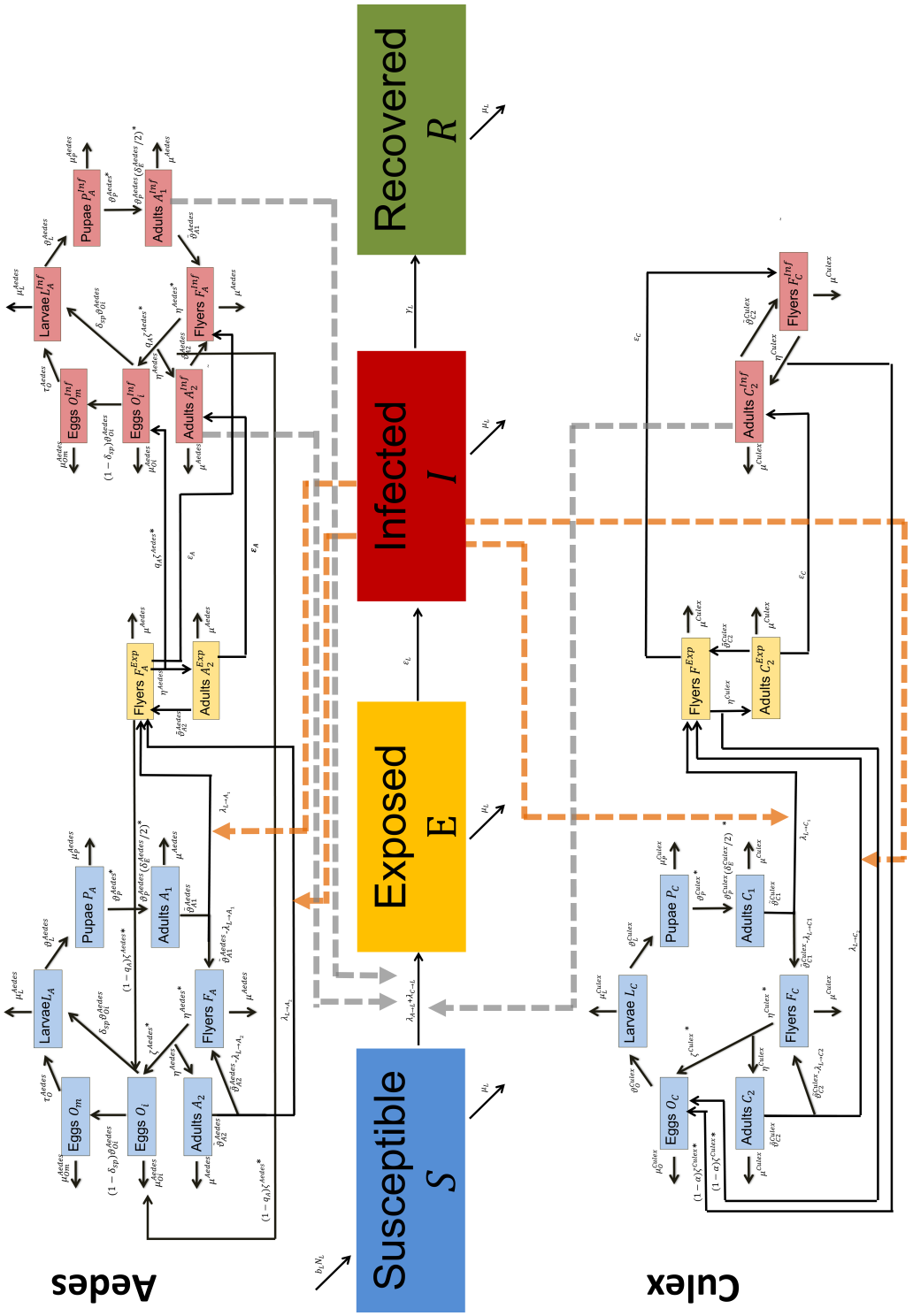

Fig. S12. Schematic representation of SEIR compartmental model for the livestock and stage-structured SEI model for the two mosquito populations for RVFV.

Fig. S13. A typical dambo in Kenya.

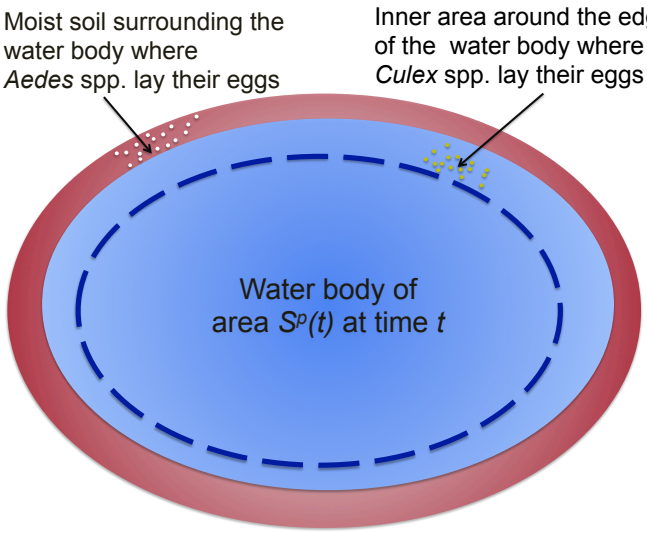

Fig. S14. Schematic illustration of breeding sites for *Aedes* sp. and *Culex* sp.

Extended technical description of results. both populations of mosquitoes establish sustained annual oscillations, while the RVFV dynamics is subjected to irregular oscillations, at least during the 30 years of simulation, (Figure S19C, mean annual surface area of water bodies $S_m^P = 5000m^2$, mean annual temperature

Impact of temperature and water bodies on the patterns of mosquitoes and RVFV population dynamics. Figure S19 shows the model predictions for the populations of susceptible and infected (exposed and infectious combined) adult *Culex* sp., adult *Aedes* sp. and livestock. All the model parameters are kept the same, except the mean annual temperature and mean annual surface area of water bodies, *i.e.* parameter T_m and S_m^P in equations Eq. (5) and Eq. (6) in the main text. The values of these two parameters impact the ecology of mosquitoes and RVFV not only quantitatively but also qualitatively, resulting in situations where both mosquitoes populations go extinct (Figure S19A, mean annual surface area of water bodies $S_m^P = 1000m^2$, mean annual temperature $T_m = 23°C$), only *Aedes* sp. go extinct (thus no trans-ovarial transmission) but *Culex* sp. establish sustained regular oscillations with an outbreak of RVFV infection (Figure S19B, mean annual surface area of water bodies $S_m^P = 3000m^2$, and, rather high, mean annual temperature $T_m = 31°C$), $T_m = 17°C$), both populations of mosquitoes and RVFV dynamics soon establish sustained regular oscillations, (Figure S19D, mean annual surface area of water bodies $S_m^P = 7500m^2$, mean annual temperature $T_m = 20°C$), both populations of mosquitoes and RVFV dynamics establish sustained regular oscillations but with marked multi-annual peaks, (Figure S19E, mean annual surface area of water bodies $S_m^P = 4000m^2$, mean annual temperature $T_m = 29°C$), and finally when both populations of mosquitoes establish sustained regular oscillations but no epidemics of RVFV infections occur, (Figure S19D, mean annual surface area of water bodies $S_m^P = 2500m^2$, mean annual temperature $T_m = 23°C$). The double annual peak usually occur for very highy temperatures. The peak in mosquito population is limited by the mean surface area of water bodies.

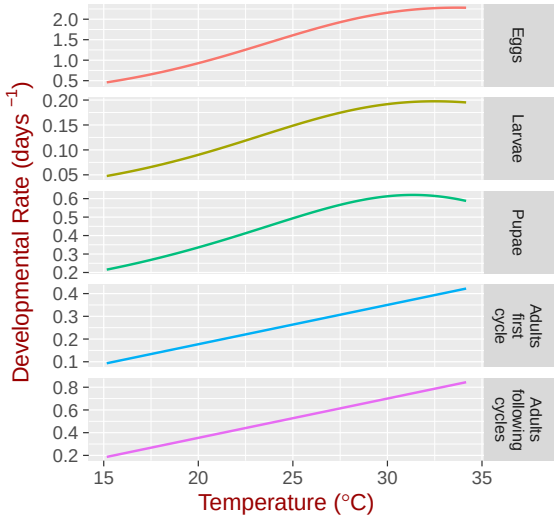

Fig. S15. Developmental rate for the different stages of *Culex* sp. according to equation Eq. (14) for different values of temperature

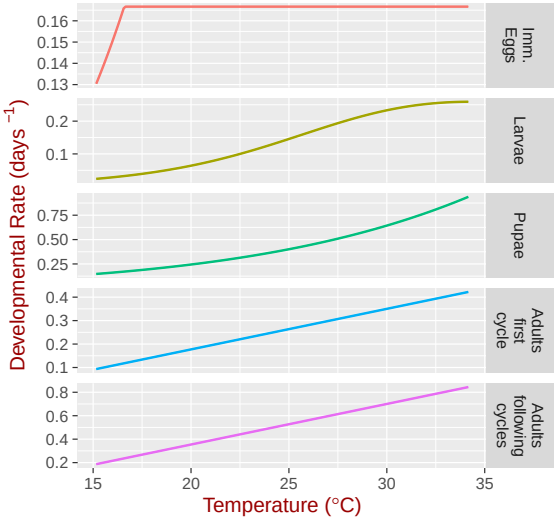

Fig. S16. Developmental rate for the different stages of *Aedes* sp. according to equation Eq. (21) for different values of temperature

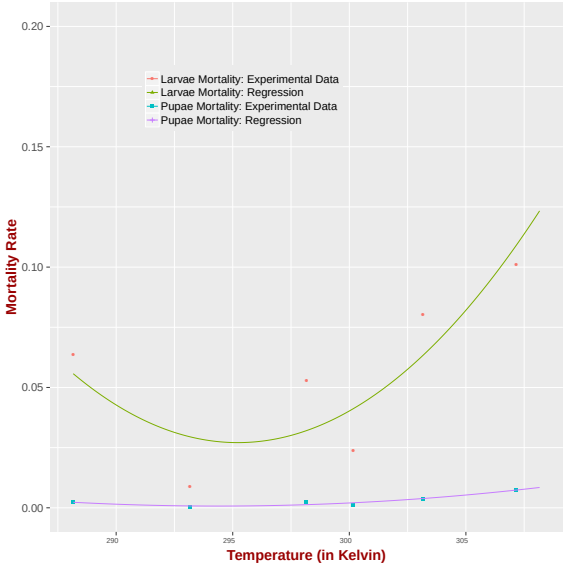

Fig. S17. Larvae and pupae mortality rates *vs* temperature for *Aedes* sp. in laboratory settings, derived from data in (14)

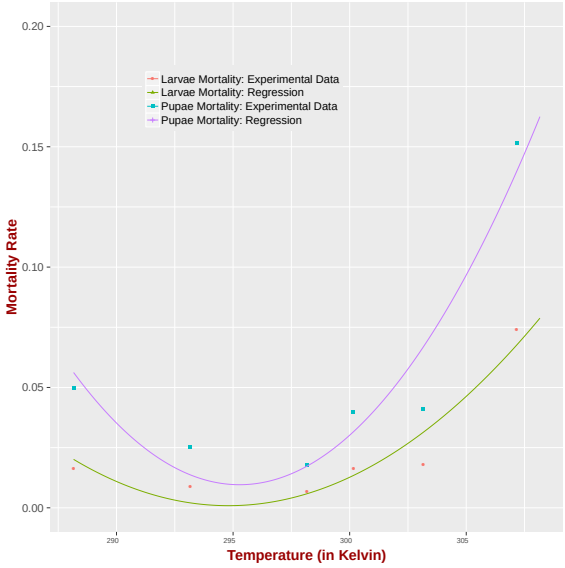

Fig. S18. Larvae and pupae mortality rates *vs* temperature for *Culex* sp. in laboratory settings, derived from data in (14)

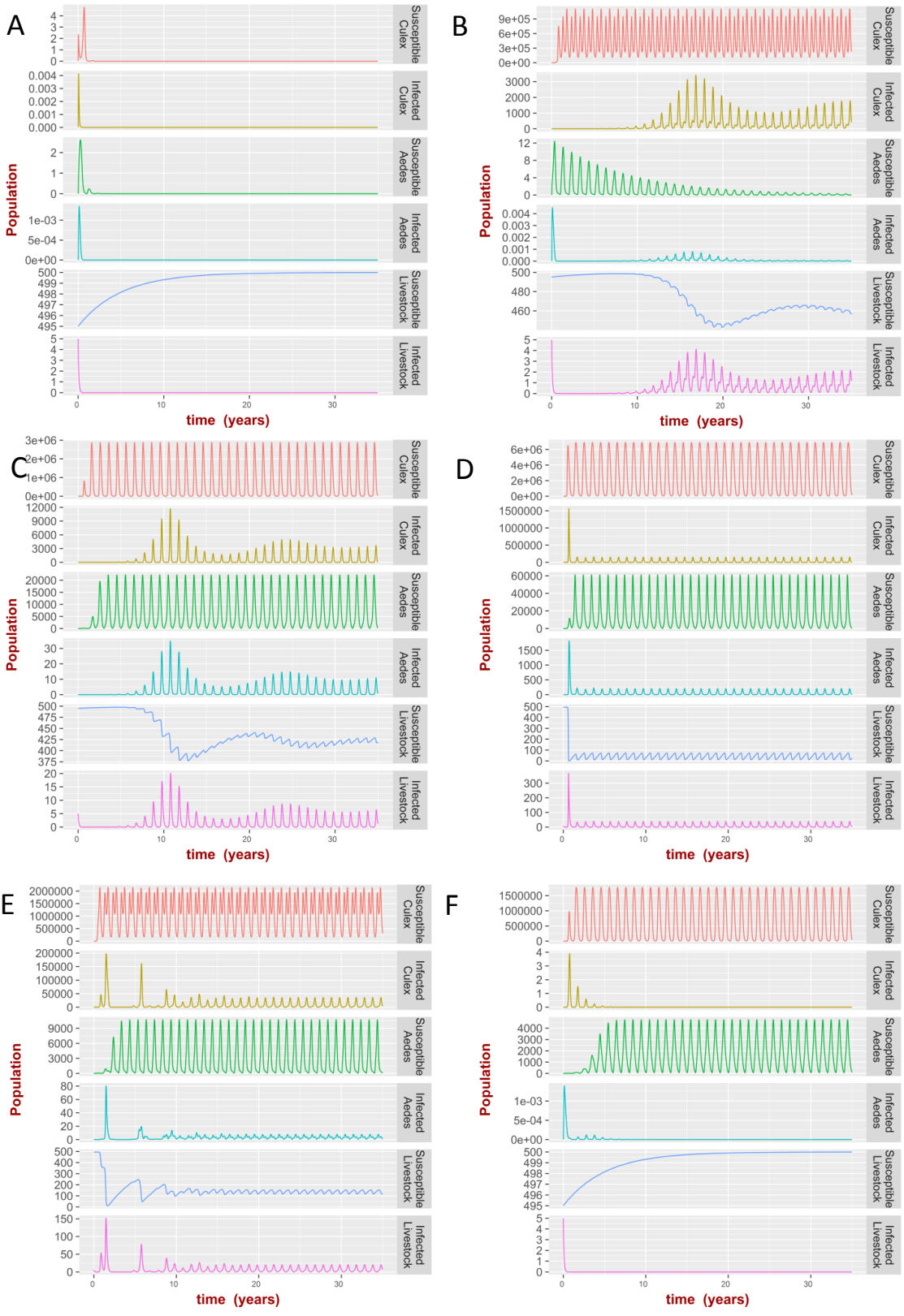

Fig. S19. Dynamics of mosquitoes population and RVFV infection in livestock. Each facet plot shows (from top to bottom) model predictions for time series of the number of susceptible and infected *Culex* sp., susceptible and infected *Aedes* sp., susceptible and infected and exposed livestock. See section 'Impact of temperature and water bodies on the patterns of mosquitoes and RVFV population dynamics' for the values of the parameters used in the simulations

Impact of water bodies fluctuations on *Aedes* sp. population. In the extreme case of no water body fluctuation, *Aedes* sp. is expected to go extinct as eggs need to be submerged to hatch. This does not always occur as a proportion of *Aedes* sp. eggs (19.7%) hatch spontaneously without flooding (7). To investigate whether or not water body fluctuations are necessary for the establishment of *Aedes* population we run the model in absence of such fluctuations. For large *constant* surface area of water bodies, (*i.e.* large oviposition rate η^{Aedes}) the proportion of eggs spontaneously hatching can reach a significant population (Fig. S20.B), even in absence of fluctuations in water body surface.

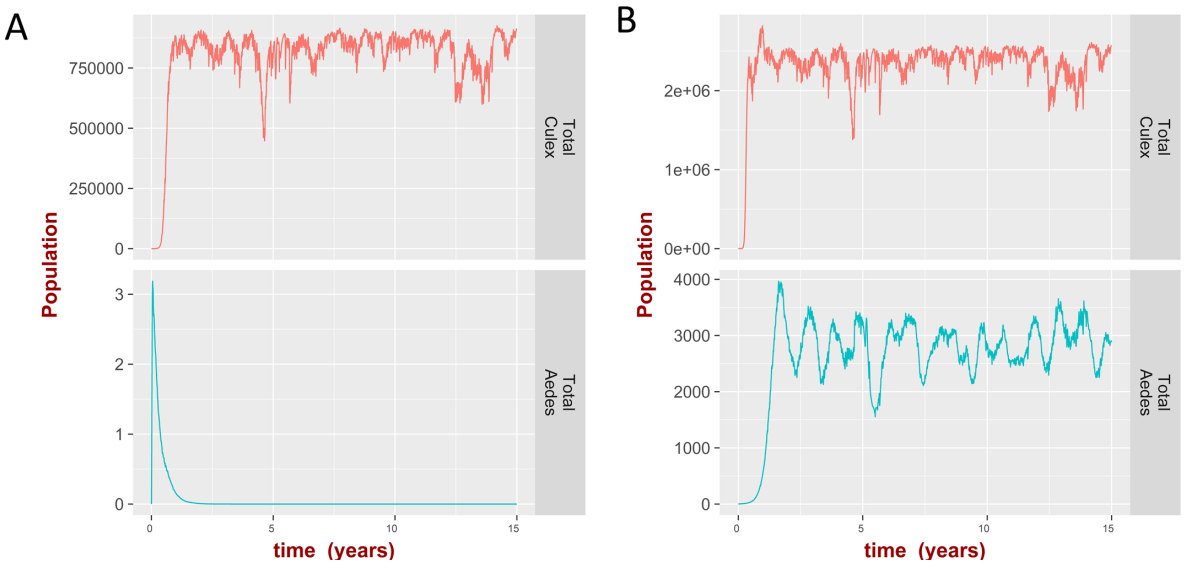

Fig. S20. Predictions of mosquitoes and RVFV when in absence of water bodies fluctuations, *i.e.* the surface area of water bodies is kept constant at any time. Temperature based on the realistic case. A) surface area of water bodies $2500\ m^2$ B) surface area of water bodies $5000\ m^2$.

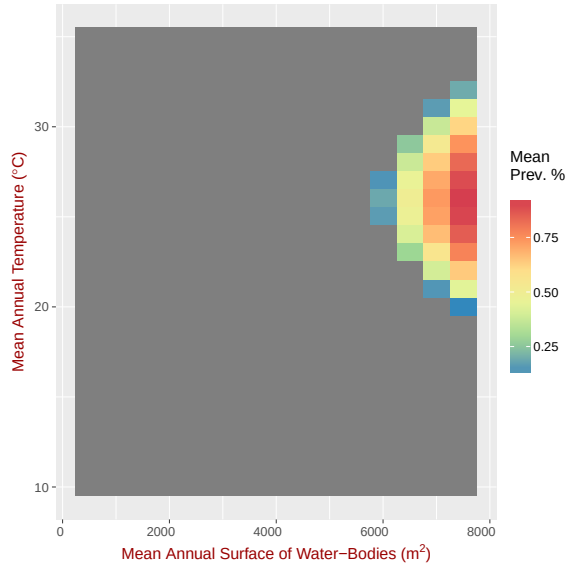

Fig. S21. As in Fig. 1, but the population of livestock is 5000 rather than 500, the infection prevalence used as initial conditions is the same in both cases (1%)

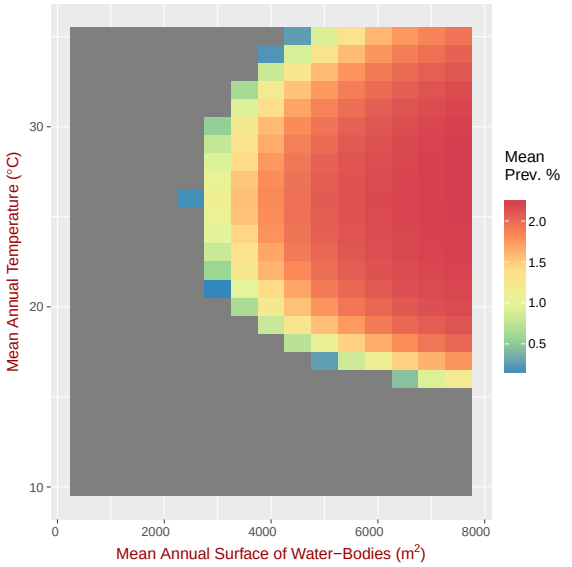

Fig. S22. As in Fig. S21, but we imposed the same vector-to-host ratio as in Fig. 1 (*i.e.* when the number of livestock is 500).

Impact of density of livestock on the RVFV infection. In the following simulation (Fig. S21) the population of livestock is 5000 rather than 500. The abundance of mosquitoes is essentially fixed by environmental factors (water body surface area and temperature) while the the number of livestock has a smaller impact. Therefore the vector-to-host ratio, and thus the prevalence, decreases for large number of livestock (dilution effect) resulting in smaller infection prevalence. In contrast, if we impose that the vector-to-host ratio is the same as in Fig. 1 (*i.e.* when the number of livestock is 500), the prevalence is slightly increased due to larger number of susceptibles (Fig. S22). Here we assumed that the presence of livestock and other animals has no impact on the spatial dispersal of the mosquitoes, however, Co_2 emitted by the animals might attract mosquitoes from neighbor areas resulting in complex, density dependent vector-to-host ratio relationships (19), largely impacting on the infection prevalence.

The potential impact of livestock density on mosquitoes population and RVFV infection. In the simulations done so far the number of livestock has a negligible effect on the biting rate and oviposition, unless the number is close to zero. This because in the correction term (10) $1/[1+(m_A)/q] \approx 1/[1+(m_C)/q] \approx 1/[1+(m_A+m_C)/q] \approx 1$ as we used the large value $q = 1E11$. In Figure S23 we used the value $q = 35$ and therefore the biting and oviposition rate strongly depends on the number of livestock with substantial impact on mosquitoes population and RVFV infection.

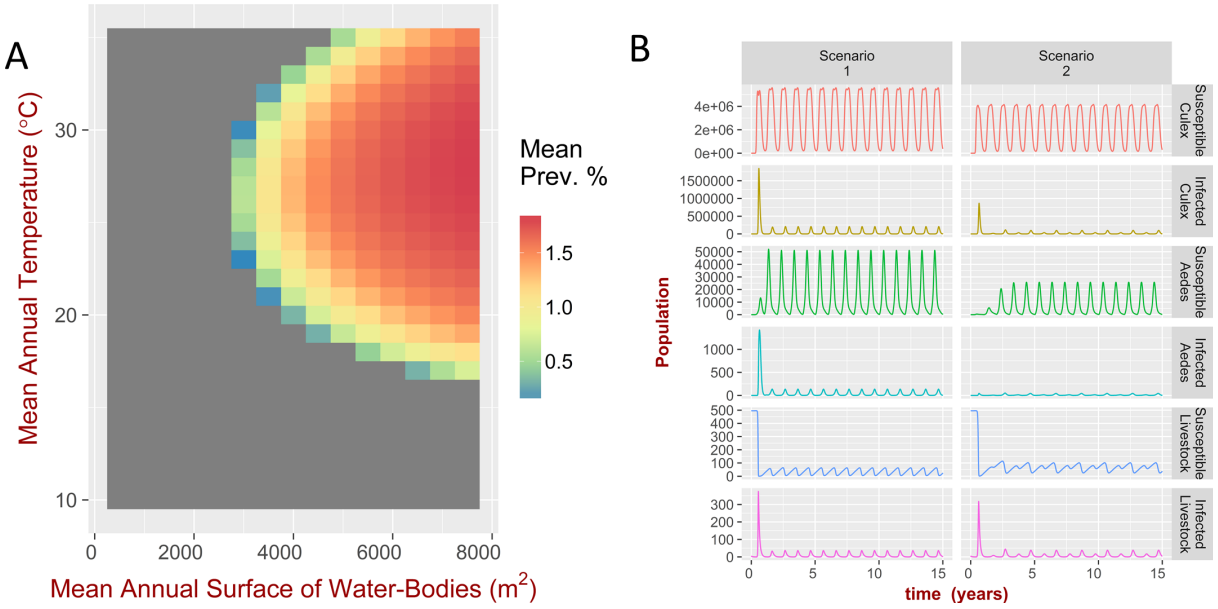

Fig. S23. A) As in Fig. 1.C, but the value of $q = 35$ rather than $q = 1E11$ in the biting rate (10) B) Dynamics of mosquitoes population and RVFV infection in livestock for $q = 1E11$ (Scenario 1) and $q = 35$ (Scenario 2l), mean surface area of water bodies $S_m^P = 7000\ m^2$, mean temperature $T_m = 25°$.

Impact of intensity of fluctuations on water bodies surface area and temperature on the RVFV infection. Figure S24 shows the impact of intensity of fluctuations on water bodies surface area and temperature on the RVFV infection. In this analysis, the parameters were chosen as the one in Fig. 1, except that the largest amplitudes in water bodies surface area and temperature (parameters S_A^P and T_A in equations Eq. (5) and Eq. (6) in the main text) were 15% of their mean values rather than 40% and 35%.

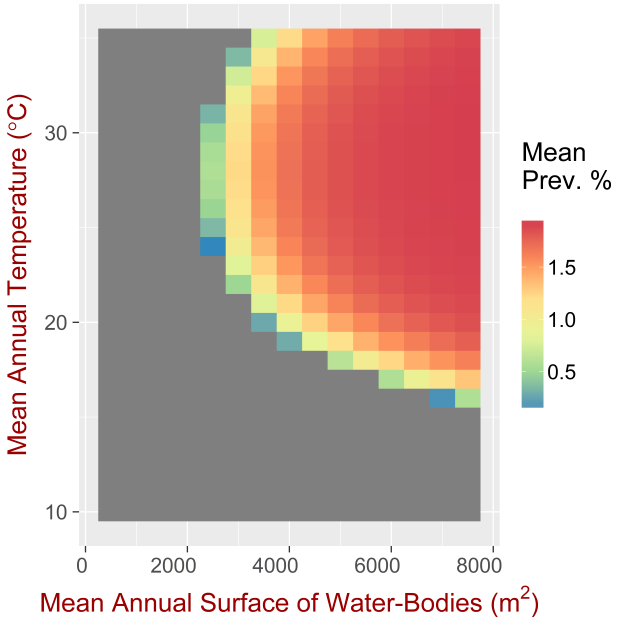

Fig. S24. As in Fig. 1, but the largest amplitudes in water bodies surface area and temperature is 15% of their mean values rather than 40% and 35%.

Impact of initial conditions on limit cycles for mosquitoes population and RVFV prevalence. Figure S25 shows the impact of initial conditions on limit cycles for mosquitoes population and RVFV prevalence. Panel A-C-E display the predictions for the theoretical model. The mean annual temperature was $T_m = 25°$ and the mean annual water bodies surface $S_m^P = 4000m^2$. In panel S25.A the initial conditions for exposed and removed livestock and all mosquitoes stages are set to zero except for susceptible and infected livestock $S_L = 495$ and $I_L = 5$ and mosquitoes eggs $O_C = 100$, $O_I = 100$ In panel S25.C, the initial conditions for exposed and removed livestock and all stages are set to zero except for susceptible livestock $S_L = 990$, for infected $I_L = 10$ and mosquitoes eggs $O_C = 100$, $O_I = 100$. In panel S25.E, the initial conditions for exposed and removed livestock are set to zero, all stages are set to 0, susceptible livestock $S_L = 9900$, for infected $I_L = 100$ and mosquitoes eggs $O_C = 100$, $O_I = 100$. Figure S25.B, S25.D and S25.F shows the predictions for the realistic model with the same initial conditions as in panels A,C,E.

Asymptotic behaviour for mosquitoes population and infection prevalence for different regimens. During the time of simulation (32 years), the mean surface area of water bodies and mean temperature is cyclic changing according the path A and path B illustrated in the panel in Fig S26.A, in contrast with the situation shown in Fig. 2, the parameter $p_f = 1$ and $\kappa^{\text{Aedes}} = \kappa^{\text{Culex}} = 0.005$ (instead of $p_f = 0.01$ and $\kappa^{\text{Aedes}} = \kappa^{\text{Culex}} = 0.001$). Temperature and surface area of water bodies are still described by the sinusoidal functions as in equations Eq. (5)-Eq. (6) in the main text, but the mean values T_m and S_m^P changes year by year (see below). The asymptotic behaviour of both the mosquitoes population and the infection prevalence is different for the different scenarios.

Timeseries of mean surface area of water bodies and mean temperature according the path A and path B. Figure S27 shows the values of the mean surface area of water bodies (S_m^P) and mean temperature (T_m) as explicit function of time for a 4−year cycle as applied in the simulation in Fig. 2. For Fig. S26, the timeseries of temperature and surface area of water bodies are qualitatively the same but not quantitatively (see caption in the figure).

Impact of phase difference. In all the simulations considered here surface area of water bodies and temperature fluctuate in phase. In this next exemplary case we considered the situation when there is a delay (or anticipation) between the times when the peaks in temperature and surface area of water bodies occur. The frequency is kept the same. Fig S28 shows the region in the space of parameters when the system results in persistent and non-persistent regimens for the population of *Culex* sp., *Aedes* sp. and RVFC prevalence, for different values of the mean annual surface of water bodies and different values of the phase difference, *e.g.* different values in the parameters ϕ_S and ϕ_T in equations Eq. (5) and Eq. (6) in the main text, resulting in the difference $\phi_S - \phi_T$ (showed in the y-axis). The figure shows that, in contrast with the population of *Aedes* sp., the population of *Culex* sp. and the prevalence of RVFV in livestock are largest when temperature and surface area of water bodies are out of phase, *e.g.* when the temperature reaches its maximum at the same time when surface area of water bodies reaches its minimum.

Impact of detection threshold on the intermittent nature of RVFV. The distribution of the length of inter-epidemics periods are expected to depend on the detection threshold, as large threshold means many epidemics goes undetected and therefore longer inter-epidemics periods. This is shown in Fig. S29. The situation when the threshold of detection is 1% of infection prevalence (rather than a fixed number of infected animals) is also shown. The model predictions are compared with historical data of RVF epidemics occurred in Kenya from 2004 to 2013. Nevertheless, due to the nature of RVF and the findings of our work, we cannot expect, at this stage, accurate matching with outbreak data for the following reasons:

- Although we have put large effort to increase the realism of the model, we are still considering only one host, while we know that many hosts, including wildlife for which data are very rare, are involved in the transmission of RVFV.
- A key finding of the current model is that the patterns of RVFV, even qualitatively, depend on the knowledge of the number of livestock, which is not currently available to us.
- The detection threshold is unknown and it is expected to randomly change in different situations.
- There are still many parameters that are not accurately known, *e.g.* dispersal parameters for the mosquitoes, impact of livestock on the host-seeking behavior of the mosquitoes etc.
- Until the points above are accurately addressed, we cannot rule out that the Kenya situation is in the unstable regime (*i.e.* the situation exemplified by path B in Fig. 1.C)
- Here we used a deterministic model, therefore the findings are strictly valid when we can meaningfully average over many realizations. The comparison of Fig. 4 and Fig. S29 demonstrates the impact of stochasticity in detection. Demographic stochasticity is also expected to play a similar role. Also, for simplicity data on water-bodies and temperature were spatially aggregated. Therefore random variation in the number of infected and in the ability to detect them will have an impact of the distribution of the inter-epidemics periods. Ideally, comparison of the model with empirical data ought to include stochastic and spatial variability.

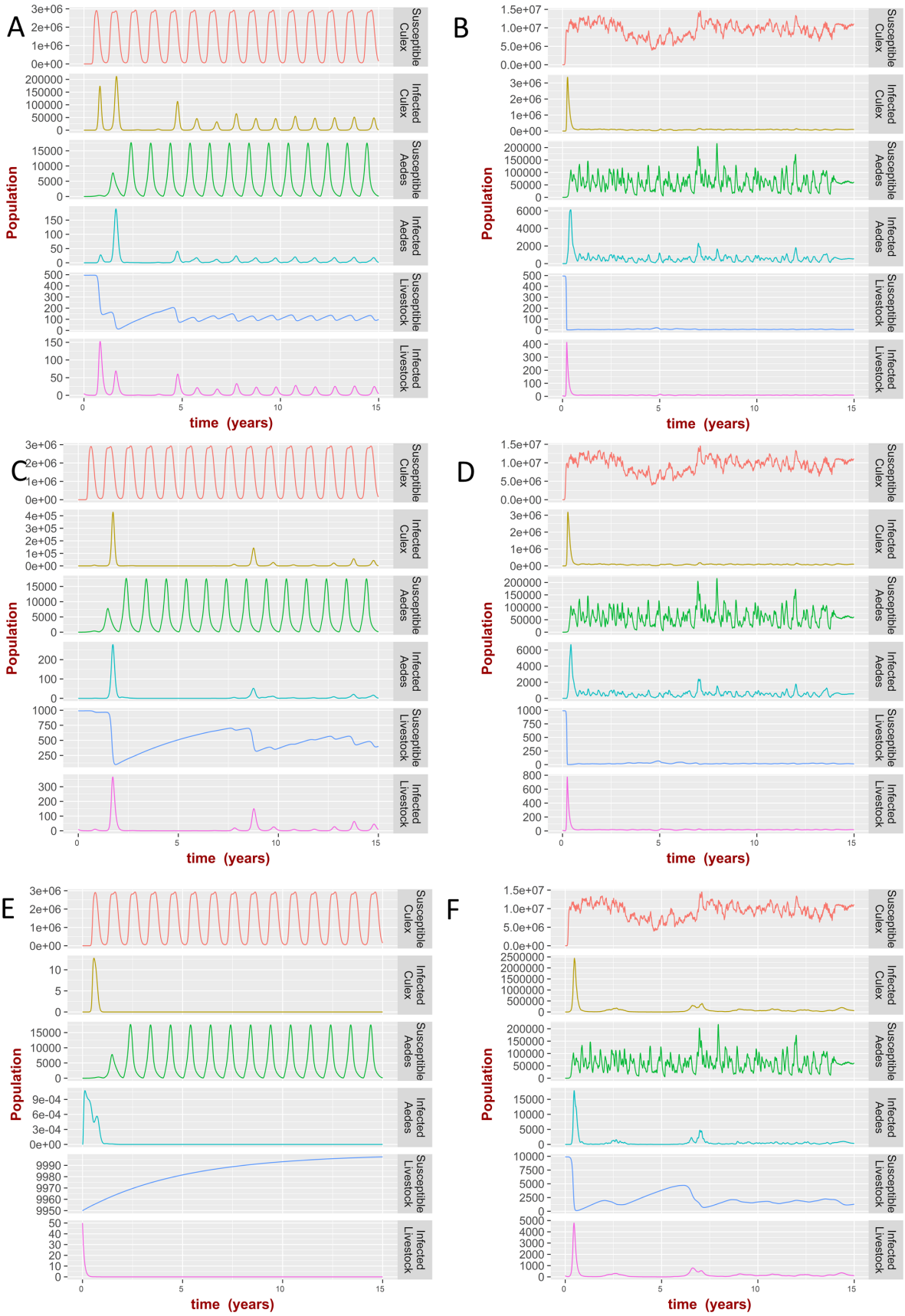

Fig. S25. Impact of initial conditions on the dynamics of mosquitoes population and RVFV infection in livestock.

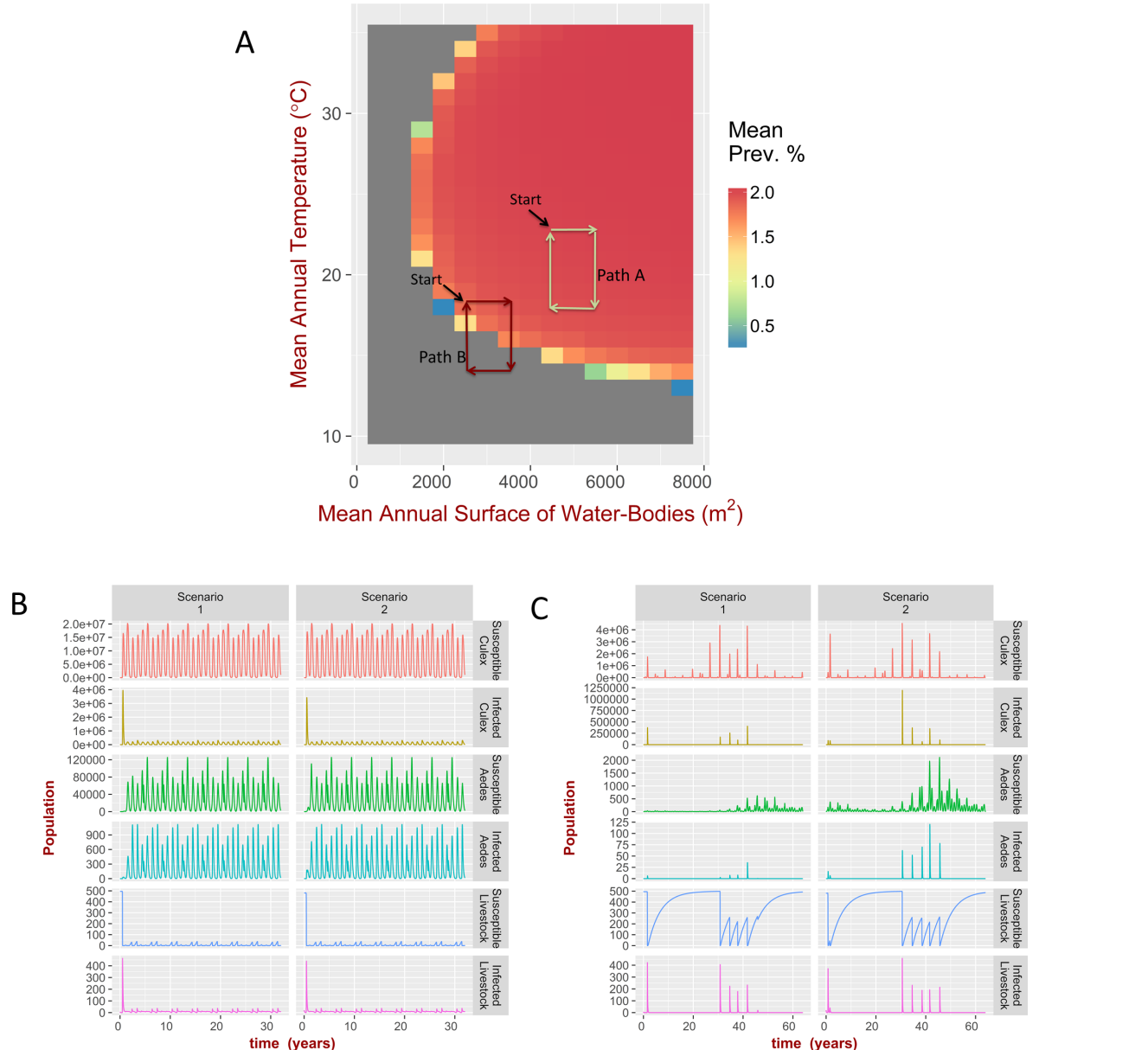

Fig. S26. A) As in Fig. 2, but $p_f = 1$, $\kappa^{\text{Aedes}} = \kappa^{\text{Culex}} = 0.005$ and during the time of simulation (32 years), the mean surface area of water bodies and mean temperature is cyclic changing according the path A and path B illustrated in the panel; *i.e.* for path A: the first year days the mean surface area of water bodies increases from $4500m^2$ to $5500m^2$ and the mean temperature is constant at 23°, followed by a second year with constant mean surface area of water bodies at $5500m^2$ while the mean temperature is decreasing from 23° to 18°, during the third year the mean surface area of water bodies decrease from $5500m^2$ to $4500m^2$ and the mean temperature is constant at 18°, followed by a fourth year when the mean temperature is increasing from 18° to 23° and the mean surface area of water bodies is constant at $4500m^2$; for path B: the dynamics is the same for path A but the range of the mean surface area of water bodies is between $2500m^2$ and $3500m^2$ and for mean temperature the range is between 14.5° and 18.5°. The variations in mean surface area of water bodies and mean temperature occur in a step-wise fashion. B) Dynamics of mosquitoes population and RVFV infection in livestock when mean temperature and mean surface area of water bodies changes according to path A, for two different initial conditions: Scenario 1) Exposed and removed livestock and all mosquitoes stages are set to zero except for susceptible and infected livestock $S_L = 495$ and $I_L = 5$ and mosquitoes eggs $O_C = 100$, $O_{A1} = 100$ Scenario 2) Exposed and removed livestock and all mosquitoes stages are set to zero except for susceptible and infected livestock $S_L = 480$ and $I_L = 20$ and mosquitoes eggs $O_C = 1000$, $O_{A1} = 1000$. The asymptotic behavior is the same in both scenarios (note that the scales on the y-axis can be different). C) as in B) but the mean temperature and mean surface area of water bodies changes according to path B. The asymptotic behaviour (even for the mosquitoes population and not only for the infection prevalence) is different for the different scenarios.

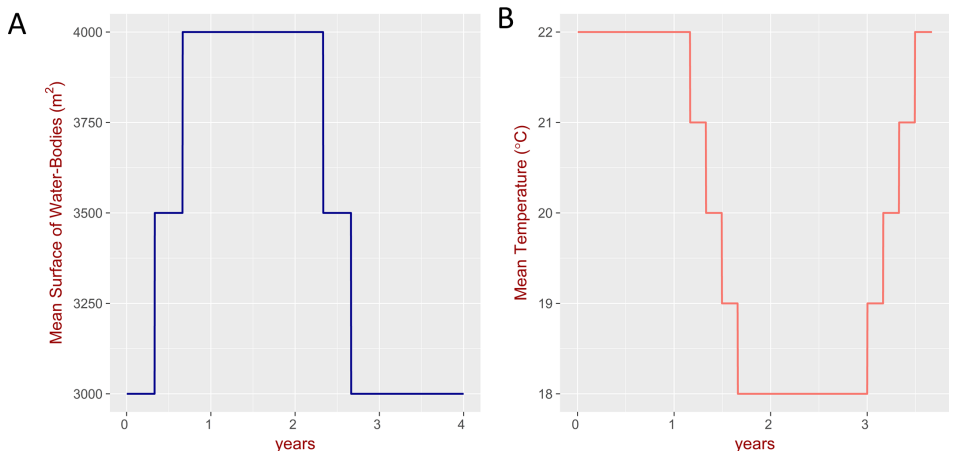

Fig. S27. Values of the mean surface area of water bodies (A) and mean temperature (B) as explicit function of time to describe the situations represented by path B in Fig. 1.C. for a $4-$year period.

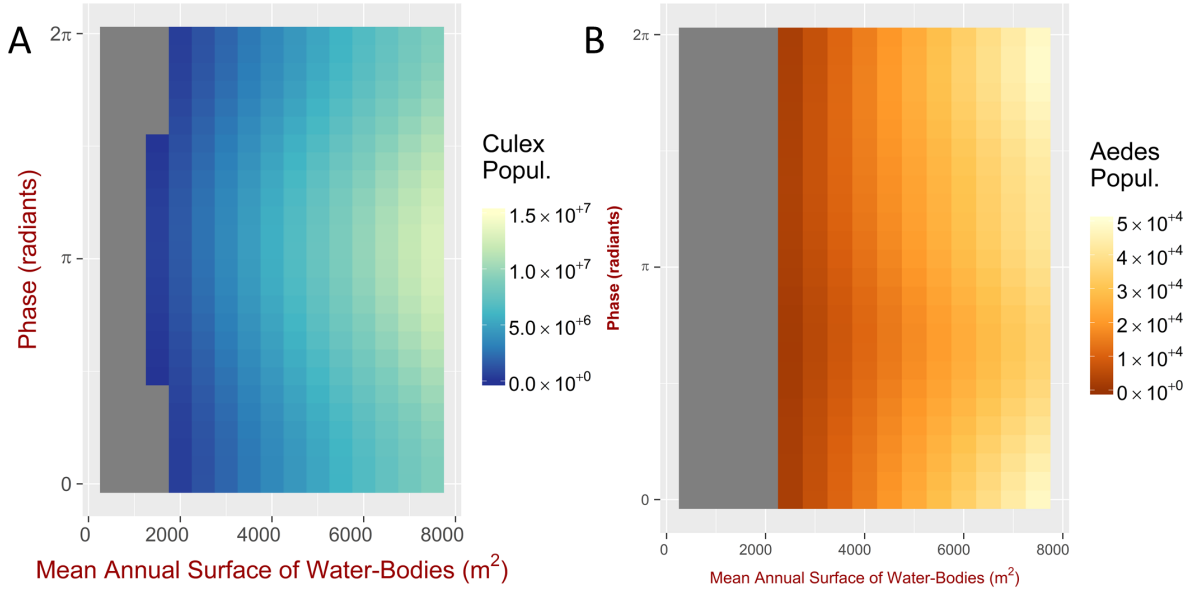

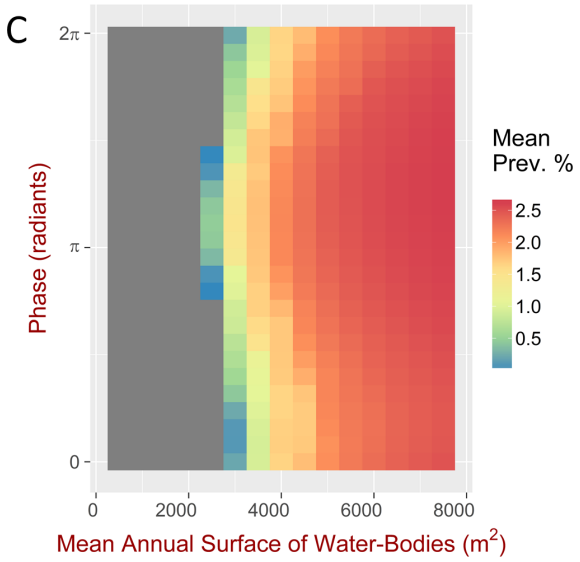

Fig. S28. Impact of phase difference between water bodies surface area and temperature on the : A) population of *Culex* sp. B) *Aedes* sp. and C) RVFV prevalence . Water bodies surface area and temperature are described by sinusoidal functions according to equation $\mathrm{Eq.}\ (5)$ and $\mathrm{Eq.}\ (6)$ in the main text. The $x-$axis shows the mean water bodies surface area S_m^P while the $y-$axis the phase in radiant. Mean value of temperature $25^\circ C$.

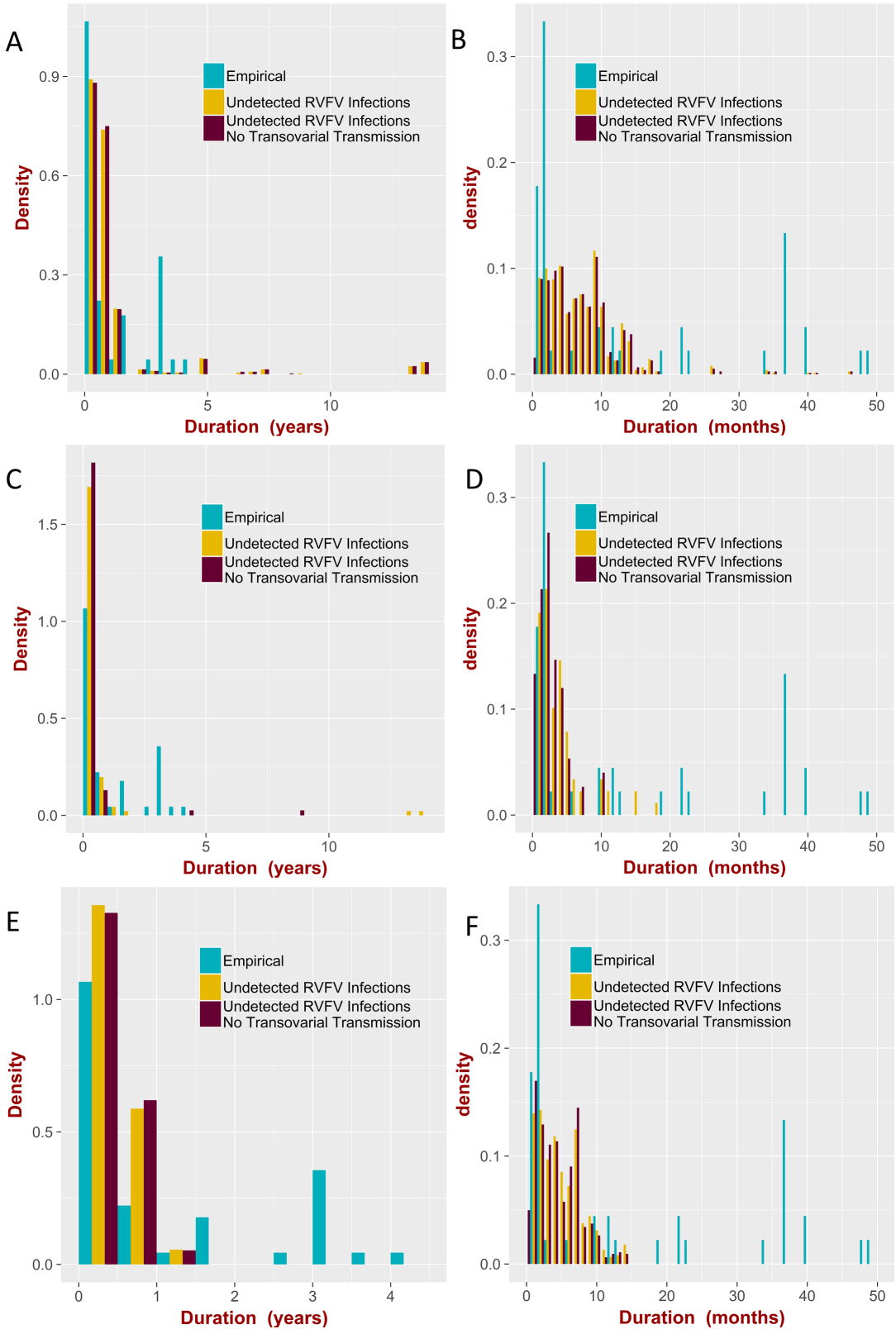

Fig. S29. A) As in Fig. 4 and presented here only for comparison (threshold of detection is 50 infected animals); C) As in Fig. 4, but the threshold of detection is 5 infected animals; E) As in Fig. 4, but the threshold of detection is 1% of infection prevalence. Panels B) D) F) visualization of the first 50 months of the corresponding panels A), C) and E).

Stability analysis for seasonal systems: Floquet theory. A key objective of the current work is to investigate the conditions that lead the ecosystem into an endemic equilibrium and whether or not this equilibrium is stable, *i.e.* whether or not small perturbations in the initial conditions will lead to the same equilibrium (20). The problem is rather challenging for RVFV, since the complex seasonalities of the system. Periodic changes in the surface of water bodies rainfall results will impact the demography of the mosquitoes and periodic changes in the temperature will impact the mortality, developmental rates, biting rate of the mosquitoes, and the extrinsic incubation period. Floquet analysis (21, 22) is a suitable approach to to test the stability of a solution. Below we show the practical procedure, the reader interested in a more rigorous aspects of the theory is referred to (22).

For simplicity, let us consider the *Culex* sp. population model in absence of disease represented by the system of differential equations Eq. (1). It is convenient to re-write the system of equations as an autonomous system, and to explicitly express the coefficients as functions of the time-dependent temperature $T(t)$ and time-dependent water bodies surface $S^P(t)$:

$$\begin{aligned}
\frac{\mathrm{d}O_C}{\mathrm{d}t} &= f_1 = \frac{b_C}{(1+p_f\frac{C_1+C_2}{qN_L})}\eta^{\text{Culex}}[S^P(t)]\left(1-\frac{O_C}{K_C[S^P(t)]}\right)F_C - \mu_O^{\text{Culex}}[T(t)]O_C - \theta_O^{\text{Culex}}[T(t)]O_C \\
\frac{\mathrm{d}L_C}{\mathrm{d}t} &= f_2 = \theta_O^{\text{Culex}}[T(t)]O_C - \mu_L^{\text{Culex}}[T(t)]L_C - \theta_L^{\text{Culex}}[T(t)]L_C \\
\frac{\mathrm{d}P_C}{\mathrm{d}t} &= f_3 = \theta_L^{\text{Culex}}[T(t)]L_C - \mu_P^{\text{Culex}}[T(t)]P_C - \theta_P^{\text{Culex}}[T(t)]P_C \\
\frac{\mathrm{d}C_1}{\mathrm{d}t} &= f_4 = \frac{1}{2}\theta_P^{\text{Culex}}[T(t)]\delta_E^{\text{Culex}}P_C - \mu_C^{\text{Culex}}[T(t)]C_1 - \tilde{\theta}_{C1}^{\text{Culex}}[T(t)]C_1 \\
\frac{\mathrm{d}F_C}{\mathrm{d}t} &= f_5 = \tilde{\theta}_{C1}^{\text{Culex}}[T(t)]C_1 + \tilde{\theta}_{C2}^{\text{Culex}}[T(t)]C_2 - \eta^{\text{Culex}}[S^P(t)]F_C - \mu_C^{\text{Culex}}[T(t)]F_C \\
\frac{\mathrm{d}C_2}{\mathrm{d}t} &= f_6 = \eta^{\text{Culex}}[S^P(t)]F_C - \mu_C^{\text{Culex}}[T(t)]C_2 - \tilde{\theta}_{C2}^{\text{Culex}}[T(t)]C_2 \\
\frac{\mathrm{d}t}{\mathrm{d}t} &= f_7 = 1
\end{aligned} \tag{32}$$

As Floquet analysis deals with systems of differential equations with periodic coefficients, we assume that the temperature $T(t)$ and surface of water bodies $S^P(t)$ are periodic functions (which in many case is justifiable by approximating temperature and surface of water bodies with the first harmonics from wavelet decomposition, see section "Empirical patterns in temperature and water bodies for Kenya" in S1 Text):

$$\begin{aligned}
S^P(t) &= S_m^P + S_A^P\cos(\omega_S t + \phi_S) \\
T(t) &= T_m + T_A\cos(\omega_T t + \phi_T)
\end{aligned} \tag{33}$$

where, as already said, ω_S and ω_T are the frequencies of oscillations in surface areas of water bodies and temperature, the terms S_m^P and T_m represent the mean surface area of water bodies and mean temperature during a period $2\pi/\omega_S$ and $2\pi/\omega_T$ respectively, S_A^P and T_A are the maximum amplitude in the oscillations and ϕ_S and ϕ_T are the phases for surface areas of water bodies and temperature respectively.

We assume that the periods $2\pi/\omega_S$ and $2\pi/\omega_T$ are equal or one is a multiple integer of the other (*e.g.* 6 months and 1 year). Thus all the coefficients in the system of equations Eq. (32) are periodic, with minimal period $T = \min(2\pi/\omega_S, 2\pi/\omega_T)$. The system of equations Eq. (32), however, is non-linear. Therefore before applying Floquet analysis to test the stability of the solutions, we need to linearise the the system. To do this we need to define the Jacobian matrix of eqn. Eq. (32):

$$\mathbf{J}_{ij} = \frac{\partial f_i}{\partial X_j}. \tag{34}$$

where $X = (O_C, L_C, P_C, C_1, F_C, C_2)$ is the vector of state variables and $f_1, f_2..$ are the explicit functions in equation Eq. (32). The Jacobian is then evaluated at the solutions (either the trivial solution leading to extinction of mosquitoes or periodic oscillations) of the system of equations Eq. (32). Then we calculate the Floquet multipliers by solving the matrix differential equation:

$$\frac{\mathrm{d}X}{\mathrm{d}t} = J(t)X \tag{35}$$

over one period (from $t = 0$ to $t = T$), with the identity matrix I as initial condition ($X(0) = I$). The matrix of the solutions at time $t = T$, $X(T)$, is known as a fundamental matrix , the Floquet multipliers, ρ_i, are the eigenvalues of $X(T)$. If all Floquet multipliers have real parts between -1 and 1 then the solution is stable.

The same approach was used for *Aedes* sp. population model in absence of disease (equation 2). The approach could be used for the system in presence of RVFV (equation 24), however due to the large number of state variables, identifying and evaluating the Jacobian over the limit cycles is numerically challenging. So the stability of the solutions was only tested numerically for a limited number of cases (*i.e.* trying different initial conditions and checking that the asymptotic solution is the same).

SI Tables.

Table S1. Type of model, theoretical or realistic, used in the figures and simulations

Figure	Type of Model
1	Theoretical
2	Theoretical
3	Realistic
4	Realistic
S19	Theoretical
S20	Realistic
S21	Theoretical
S22	Theoretical
S23	Theoretical
S24	Theoretical
S25.A S25.C S25.E	Theoretical
S25.B S25.D S25.F	Realistic
S26	Theoretical
S27	Theoretical
S28	Theoretical
S29	Realistic

Table S2. State Variables

Symbol	State Variable	Mosquito Species	Epidemiological State
O_C	Egg population	*Culex* sp.	Susceptible
L_C	Larva population	*Culex* sp.	Susceptible
P_C	Pupa population	*Culex* sp.	Susceptible
C_1	Nulliparous female, *i.e.* female adults not having laid eggs	*Culex* sp.	Susceptible
F_C	fFyers, *i.e.* adult female in search of breeding sites	*Culex* sp.	Susceptible
C_2	Female adults having laid eggs	*Culex* sp.	Susceptible
F_C^{Exp}	Flyers, *i.e.* adult female in search of breeding sites	*Culex* sp.	Exposed
C_2^{Exp}	Female adults having laid eggs	*Culex* sp.	Exposed
F_C^{Inf}	Flyers, *i.e.* adult female in search of breeding sites	*Culex* sp.	Infectious
C_2^{Inf}	Female adults having laid eggs	*Culex* sp.	Infectious
O_I	Immature egg population	*Aedes* sp.	Susceptible
O_M	Mature egg population	*Aedes* sp.	Susceptible
L_A	Larva population	*Aedes* sp.	Susceptible
P_A	Pupa population	*Aedes* sp.	Susceptible
A_1	Nulliparous female, *i.e.* female adults not having laid eggs	*Aedes* sp.	Susceptible
F_A	Flyers, *i.e.* adult female in search of breeding sites	*Aedes* sp.	Susceptible
A_2	Female adults having laid eggs	*Aedes* sp.	Susceptible
F_A^{Exp}	Flyers, *i.e.* adult female in search of breeding sites	*Aedes* sp.	Exposed
A_2^{Exp}	Female adults having laid eggs	*Aedes* sp.	Exposed
O_I^{Inf}	Immature egg population	*Aedes* sp.	Infectious
O_M^{Inf}	Mature egg population	*Aedes* sp.	Infectious
L_A^{Inf}	Larva population	*Aedes* sp.	Infectious
P_A^{Inf}	Pupa population	*Aedes* sp.	Infectious
A_1^{Inf}	Nulliparous female, *i.e.* female adults not having laid eggs	*Aedes* sp.	Infectious
F_A^{Inf}	Flyers, *i.e.* adult female in search of breeding sites	*Aedes* sp.	Infectious
A_2^{Inf}	Female adults having laid eggs	*Aedes* sp.	Infectious
S_L	Number of livestock	-	Susceptible
E_L	Number of livestock	-	Exposed
I_L	Number of livestock	-	Infectious
R_L	Number of livestock	-	Recovered
N_L	Number of livestock	-	Total ($S_L+E_L+I_L+R_L$)

Table S3. Parameters: *Culex* sp. Temperature measured in Kelvin K, rates calculated per day, dimensions are expressed in length (L) and time (T).

Parameter	Symbol and Dimension	Information
Number of eggs laid per batch	b_C, [−]	200, estimate for *Culex poicilipes* (23). It assumes unlimited blood meals.
Density dependent number of eggs laid per batch	$\tilde{b}_C$, [−]	It include a dependency on the number of livestock, as mosquitoes cannot produce eggs without ingesting blood meals. See Eq. (6).
Parameter for the impact of the livestock on vector fecundity and gonotrophic cycles (or biting rate)	q, [−]	$q = 1E11$, $q = 35$. This parameter takes into account that in absence of host, *i.e.* no blood-meal, the number of eggs per batch and the gonotrophic cycles (or biting rate) drops to zero. For large values of q, the number of livestock (unless the number is very small) has negligible impact on vector fecundity and gonotrophic cycles.
Vector-to-Host ratio	m_C, [−]	Ratio of a proportion of adults female, calculated from the model, per number of livestock. See Eq. (7) and Eq. (26).
Proportion of adults female feeding on host	p_f, [−]	$p_f = 0.01$ (except in Figure S26, where $p_f = 1$) based on the assumption that that only 1% of the entire mosquito population is able to detect and feed on the particular host species under consideration. The rest of the mosquitoes either feed on different species or die due to other causes such as predation. See Eq. (7) and Eq. (26).
Eggs maximum density per m^2	ρ_C, $[L^{-2}]$	Different estimates are available in the literature. Here we choose $\rho_C = 1.5\ 10^5$ which is of the same order of magnitude of (23).
Proportion of area of the water body where *Culex* sp. lay their eggs	κ^{Culex}, [−]	There are some indication that the inner distance from the pond border defining the laying area of *Culex* on the water is about 1m (23); however, the value $\kappa^{\text{Culex}} = 0.001$ (and $\kappa^{\text{Culex}} = 0.005$ in Figure S26) are arbitrary.
Typical area scanned by *Culex* sp. fliers.	$\mathcal{A}$, $[L^2]$	$1E6\ m^2$, based on some indication that the spatial range of the activity of mosquitoes would be up to $1500\ m$ to the nearest suitable water body (9).
Density dependent egg load rate	ξ^{Culex}, ζ^{Culex}, $[T^{-1}]$	This is a measure of the number of eggs laid by all flyers per time unit. Underlying this model is the expectation that the rate of change of the number of eggs would decrease if the breeding site is already occupied by eggs. See equations Eq. (4) also Eq. (25).
Oviposition rate (*i.e.* number of times a flyer lay a batch of eggs per time unit)	η^{Culex}, $[T^{-1}]$	The measure takes into account the typical surfaces scanned by adult flyers searching for a breeding site. See equation Eq. (3).
Carrying capacity for eggs	K_C, [−]	It takes into account that the maximum number of eggs that can be laid over a water body is limited by its surface. See equation Eq. (5).
Average time for egg deposition in laboratory conditions	t_{dep}, $[T]$	0.229 days (8).
Daily egg mortality	μ_O^{Culex}, $[T^{-1}]$	$\mu_O^{\text{Culex}} = \begin{cases} 1 - 0.97 & \text{if } T \leq 286.15K \\ 1 - [54.259\exp(-0.3114(T - 273.15)] & \text{if } 286.15K < T \leq 292.13K \\ 1 - 0.22 & \text{if } 292.13K < T \leq 303K \\ 1 - [0.0876(T - 273.15) - 2.3577] & \text{if } T > 303K \end{cases}$ (24)
Daily larva mortality	μ_L^{Culex}, $[T^{-1}]$	Based on (14), we used $\mu_L^{\text{Culex}} = 37.9318 - 0.2573T + 0.0004T^2$.
Daily pupa mortality	μ_P^{Culex}, $[T^{-1}]$	Based on (14), we used $\mu_P^{\text{Culex}} = 80.3113 - 0.54391T + 0.0009T^2$.
Daily adult mortality	μ^{Culex}, $[T^{-1}]$	0.16 based on daily survivorship of (25).
Additional pupal mortality	δ_E^{Culex}, [−]	Besides the daily mortality in the pupal stage, there is an additional mortality $\delta_E^{\text{Culex}} = 0.83$ associated with the emergence of the adult (6).
Biting rates, *i.e.* the reciprocal of the time interval between blood meals	$\tilde{\theta}_{C1}^{\text{Culex}}$, $\tilde{\theta}_{C2}^{\text{Culex}}$, $[T^{-1}]$	Assume one blood meal per oviposition, therefore this is equal to the number of gonotrophic cycles per time unit. The developmental rate for the subsequent gonotrophic cycles was assumed to be twice the developmental rate for the first gonotrophic cycle ($\theta_{C2}^{\text{Culex}} = 2\theta_{C1}^{\text{Culex}}$ (12)). The developmental rates for the first gonotrophic cycle, assuming infinite availability of blood meal resources (*i.e.* large number of livestock), depends on temperature, T, as $\theta_{C1}^{\text{Culex}} = 0.0173[(T - 273.15) - 9.6)]$ (11) The impact of livestock is incorporated according to Eq. (13) and Eq. (29).
All other developmental rates	θ_x^{Culex}, $[T^{-1}]$	Modeled according (13) and based on the data from (6, 14) listed in table S6. See equation 14 and Fig. S15.
Force of Infection: from *Culex* sp. to livestock	$\lambda_{C\to L}$, $[T^{-1}]$	Modeled according to Eq. (28).
Probability of infection following ingestion of infected blood meal: from *Culex* sp. to livestock	$\beta_{C\to L}$, [−]	$\beta_{C\to L} = 0.78$, see (11).
Extrinsic Incubation period in *Culex* sp.	$1/\epsilon_C$, $[T]$	$[-0.1038 + 0.0071(T - 273.15)]^{-1}$ (16).
Disease induced reduction in the feeding rate	α, [−]	$\alpha = 0.21$ take into account that infected *Culex Pipiens* showed a 21% reduction in the feeding rate (15).

Table S4. Parameters: *Aedes* sp. Temperature measured in Kelvin degree, rates calculated per day. Temperature measured in Kelvin K, rates calculated per day, dimensions are expressed in length (L) and time (T).

Parameter	Symbol and Dimension	Information
Number of eggs laid per batch	b_A, $[-]$	based on argument that females lay a number of eggs that is roughly proportional to their body weight (6) estimated $b_A = 63$ for *Aedes aegypti*, here we choose $b_A = 100$. It assumes unlimited blood meals.
Density dependent number of eggs laid per batch	$\tilde{b}_A$, $[-]$	It include a dependency on the number of livestock, as mosquitoes cannot produce eggs without ingesting blood meals. See Eq. (10) and Eq. (25).
Parameter for the impact of the livestock on vector fecundity and gonotrophic cycles (or biting rate)	q, $[-]$	As for *Culex* sp., we choose $1E11$ and $q = 35$. See table S3.
Vector-to-Host ratio	m_A, $[-]$	Ratio of a proportion of adults female, calculated from the model, per number of livestock. See Eq. (11) and Eq. (26).
Proportion of adults female feeding on host	p_f, $[-]$	As for *Culex* sp., we choose $p_f = 0.01$. See table S3.
Eggs maximum density per m^2	ρ_A, $[L^{-2}]$	Different estimates are available in the literature. As for *Culex* sp., we choose $\rho_A = 1.5\,10^5$. See table S3.
Proportion of area on the soil where *Aedes* sp. lay their eggs	κ^{Aedes}, $[-]$	As for *Culex* sp., the value $\kappa^{\text{Aedes}} = 0.001$ (and $\kappa^{\text{Aedes}} = 0.005$ in Figure S26) are arbitrary. See table S3.
Typical area scanned by *Aedes* sp. fliers.	$\mathcal{A}$, $[L^2]$	As for *Culex* sp., we choose $1E6\ m^2$. See table S3.
Density dependent egg load rate	ξ^{Aedes}, ζ^{Aedes}, $[T^{-1}]$	See Eq. (8) and Eq. (25) and table S3.
Oviposition rate (*i.e.* number of times a flyer lay a batch of eggs per time unit)	η^{Aedes}, $[T^{-1}]$	See Eq. (3) and table S3.
Carrying capacity for eggs	K_A, $[-]$	See equation Eq. (9) and table S3.
Average time for egg deposition in laboratory conditions	t_{dep}, $[T]$	0.229 days (8).
Daily egg mortality	μ_{Oi}^{Aedes}, $[T^{-1}]$	$\mu_{Oi}^{\text{Aedes}} = 0.0004$ crudely estimated as $1/4$ years, based on the argument that desiccated eggs can survive in the soil for several years.
Daily egg mortality	μ_{Om}^{Aedes}, $[T^{-1}]$	$\mu_{Om}^{\text{Aedes}} = 0.011$ (6).
Daily larva mortality	μ_{L}^{Aedes}, $[T^{-1}]$	Based on (14), we used $\mu_{L}^{\text{Aedes}} = 50.1205 + 0.3394T + 0.00057T^2$.
Daily pupa mortality	μ_{P}^{Aedes}, $[T^{-1}]$	Based on (14), we used $\mu_{P}^{\text{Aedes}} = 3.524873 - 2.394308 \cdot 10^{-2}T + 4.066735 \cdot 10^{-5}T^2$.
Daily adult mortality	μ^{Aedes}, $[T^{-1}]$	$[25.8 - 0.45(T - 273.16)]^{-1}$ (11).
Additional pupal mortality	δ_E^{Aedes}, $[-]$	As for *Culex* sp., we choose $\delta_E^{\text{Aedes}} = 0.83$. See table S3.
Proportion of spontaneous hatching without flooding	δ_{sp}, $[-]$	$\delta_{sp} = 0.197$ (7).
Biting rates, *i.e.* the reciprocal of the time interval between blood meals	$\tilde{\theta}_{A1}^{\text{Aedes}}$, $\tilde{\theta}_{A2}^{\text{Aedes}}$, $[T^{-1}]$	As for *Culex* sp., see Eq. (20), Eq. (29) and table S3.
Developmental rate for newly laid eggs	$\theta_{OI}^{\text{Aedes}}$, $[T^{-1}]$	See equation Eq. (15).
All other developmental rates	$\theta_{x}^{\text{Aedes}}$, $[T^{-1}]$	See equation 21, table S6, Fig. S16.
Force of Infection: from *Aedes* sp. to livestock	$\lambda_{A\to L}$, $[T^{-1}]$	Modeled according to Eq. (28).
Probability of infection following ingestion of infected blood meal: from *Aedes* sp. to livestock	$\beta_{A\to L}$, $[-]$	$\beta_{A\to L} = 0.70$, see (11).
Extrinsic Incubation period in *Aedes* sp.	$1/\epsilon_A$, $[T]$	$[-0.1038 + 0.0071(T - 273.15)]^{-1}$ (16).
Desiccation period	T_d, $[T]$	6 days (23, 26). See equation Eq. (1).
Hatching rate	τ_O^{Aedes}, $[T^{-1}]$	It depends on water bodies size and their rate of change, it is modeled as Eq. (4).
Probability of transovarial transmission	q_A, $[-]$	0.007, see (11)

Table S5. Parameters: Livestock. Rates calculated per day, dimensions are expressed in length (L) and time (T).

Parameter	Symbol and Dimension	Information
Total livestock population	N_L, [−]	$N_L = 500$ (most cases), $N_L = 1000$, $N_L = 5000$, $N_L = 10000$.
Birth rate for livestock	b_L, $[T^{-1}]$	$b_L = 1/(5 \cdot 365)$ from (16).
Livestock natural mortality	μ_L, $[T^{-1}]$	$\mu_L = 1/(5 \cdot 365)$ from (16)
Probability of infection : Livestock to *Culex* sp.	$\beta_{C\to L}$, [−]	0.22 (11)
Probability of infection : Livestock to *Aedes* sp.	$\beta_{C\to L}$, [−]	0.38 (11)
Latent period	$1/\epsilon_L$, $[T]$	$1/\epsilon_L = 3.5$ days (27)
Infectious period	$1/\gamma_L$, $[T]$	$\gamma_L = 30$ days (27))
Force of Infection: from livestock to *Culex* sp.	$\lambda_{L\to C_1}$, $\lambda_{L\to C_2}$, $[T^{-1}]$	This is a function scaling with the first and second gonotrophic cycles and modeled according to Eq. (27).
Force of Infection: from livestock to *Aedes* sp.	$\lambda_{L\to A_1}$, $\lambda_{L\to A_2}$, $[T^{-1}]$	This is a function scaling with the first and second gonotrophic cycles and modeled according to Eq. (27).

Table S6. Parameter estimates to calculate the developmental rates using Sharpe and DeMichele's model (equations Eq. (14), Eq. (21)) for *Culex quinquefasciatus* and *Aedes aegypti*. From (14). θ_x^{Culex} is measured in day^{-1}, enthalpies are measured in cal mol^{-1} and the temperature is measured in absolute (Kelvin) degrees.

Symbol	Life Stage	$\theta_x^{\text{Culex}}(298^\circ K)$	ΔH_A	$T_{1/2}$	ΔH_H
θ_O^{Culex}	First Instar	1.23439	27534.92	301.00	37071.82
θ_L^{Culex}	Larva	0.21554	24689.00	301.82	37270.21
θ_P^{Culex}	Pupa	0.55490	15648.63	306.60	43983.41
Symbol	**Life Stage**	$\theta_x^{\text{Aedes}}(298^\circ K)$	ΔH_A	$T_{1/2}$	ΔH_H
θ_O^{Aedes}	First Instar	0.68007	28033.83	304.33	72404.07
θ_L^{Aedes}	Larva	0.20429	36072.78	301.56	45543.49
θ_P^{Aedes}	Pupa	0.74423	19246.42	302.68	5954.35

Table S7. Effect of constant temperatures on *Cx. quinquefasciatus* and *Ae. aegypti* survivals and time to complete a stage.

Temperature °C	$S^{\text{Culex}}(\%)$	$S^{\text{Aedes}}(\%)$	t_L^{Culex} (days)	t_P^{Culex} (days)	t_L^{Aedes} (days)	t_P^{Aedes} (days)
15	38.15	3.11	25.35	6.03	46.83	8.49
20	85.25	91.80	9.53	2.54	9.31	3.11
25	90.30	62.58	7.95	2.33	8.61	3.03
27	84.87	89.76	5.38	1.65	4.47	1.79
30	83.12	66.34	5.41	1.79	4.99	1.82
34	42.07	59.14	5.18	1.84	5.06	1.09

Based on (14). S^{Culex} is the mean survival (%) from egg hatch to adult stage for *Cx. quinquefasciatus*. S^{Aedes} is the mean survival (%) from egg hatch to adult stage for *Ae. aegypti*. t_L^{Culex} and t_P^{Culex} are the mean number of days to complete larva and pupa stages for *Cx. quinquefasciatus*. t_L^{Aedes} and t_P^{Aedes} are the mean number of days to complete larva and pupa stages for *Ae. aegypti*.

References

1. Menne MJ, Durre I, Vose RS, Gleason BE, Houston TG (2012) An Overview of the Global Historical Climatology Network-Daily Database. *Journal of Atmospheric and Oceanic Technology* 29(7):897–910.
2. Anonymous (2016) Copernicus Global Land Service ([Internet]. Retrieved 02/06/2016, available at: http://land.copernicus.eu/global/).
3. Baret F, et al. (2006) VGT4Africa user manual First edition, (European Commission Directorate-General Joint Research Centre Institute for Environment and Sustainability), Technical report.
4. van Etten RJHJ (2012) *raster: Geographic analysis and modeling with raster data.* R package version 2.0-12.
5. Cazelles B, et al. (2008) Wavelet analysis of ecological time series. *Oecologia* 156(2):287–304.
6. Otero M, Schweigmann N, Solari HG (2008) A stochastic spatial dynamical model for Aedes aegypti. *Bulletin of mathematical biology* 70(5):1297–325.
7. Focks DA, Haile DG, Daniels E, Mount GA (1993) Dynamic life table model for Aedes aegypti (Diptera: Culicidae): analysis of the literature and model development. *Journal of medical entomology* 30(6):1003–17.
8. Christophers R (1960) *Aedes aegypti (L.), the Yellow Fever Mosquito.* (Univ. Press, Cam- bridge.).
9. Diallo D, et al. (2011) Temporal distribution and spatial pattern of abundance of the Rift Valley fever and West Nile fever vectors in Barkedji, Senegal. *Journal of vector ecology : journal of the Society for Vector Ecology* 36(2):426–36.
10. Pelosse P, et al. (2013) Influence of vectors' risk-spreading strategies and environmental stochasticity on the epidemiology and evolution of vector-borne diseases: the example of Chagas' disease. *PloS one* 8(8):e70830.
11. Fischer EA, Boender GJ, Nodelijk G, de Koeijer AA, van Roermund HJ (2013) The transmission potential of Rift Valley fever virus among livestock in the Netherlands: a modelling study. *Veterinary Research* 44(1):58.
12. Reisen WK, Fang Y, Martinez VM (2006) Effects of temperature on the transmission of west nile virus by Culex tarsalis (Diptera: Culicidae). *Journal of medical entomology* 43(2):309–17.
13. Schoolfield RM, Sharpe PJ, Magnuson CE (1981) Non-linear regression of biological temperature-dependent rate models based on absolute reaction-rate theory. *Journal of theoretical biology* 88(4):719–31.
14. Rueda LM, Patel KJ, Axtell RC, Stinner RE (1990) Temperature-dependent development and survival rates of Culex quinquefasciatus and Aedes aegypti (Diptera: Culicidae). *Journal of medical entomology* 27(5):892–8.
15. Turell MJ, Gargan TP, Bailey CL (1985) Culex pipiens (Diptera: Culicidae) morbidity and mortality associated with Rift Valley fever virus infection. *Journal of medical entomology* 22(3):332–337.
16. Barker CM, Niu T, Reisen WK, Hartley DM (2013) Data-driven modeling to assess receptivity for rift valley Fever virus. *PLoS neglected tropical diseases* 7(11):e2515.
17. Sota T, Mogi M (1989) Effectiveness of zooprophylaxis in malaria control: a theoretical inquiry, with a model for mosquito populations with two bloodmeal hosts. *Medical and Veterinary Entomology* 3(4):337–345.
18. Kelly DW, Thompson CE (2000) Epidemiology and optimal foraging: modelling the ideal free distribution of insect vectors. *Parasitology* 120 (Pt 3:319–27.
19. Lo Iacono G, Robin CA, Newton JR, Gubbins S, Wood JLN (2013) Where are the horses? With the sheep or cows? Uncertain host location, vector-feeding preferences and the risk of African horse sickness transmission in Great Britain. *J. R. Soc. Interface* 10(83):20130194–.
20. May RMRM (2001) *Stability and complexity in model ecosystems.* (Princeton University Press), second edition, p. 265.
21. Klausmeier Ca (2008) Floquet theory: a useful tool for understanding nonequilibrium dynamics. *Theoretical Ecology* 1(3):153–161.
22. Grimshaw R (1990) *Nonlinear ordinary differential equations.* (Blackwell Scientific, Oxford).
23. Soti V, et al. (2012) Combining hydrology and mosquito population models to identify the drivers of Rift Valley fever emergence in semi-arid regions of West Africa. *PLoS neglected tropical diseases* 6(8):e1795.
24. Morin CW, Comrie AC (2010) Modeled response of the West Nile virus vector Culex quinquefasciatus to changing climate using the dynamic mosquito simulation model. *International journal of biometeorology* 54(5):517–29.
25. Reisen WK, Milby MM, Presser SB, Hardy JL (1992) Ecology of mosquitoes and St. Louis encephalitis virus in the Los Angeles Basin of California, 1987-1990. *Journal of medical entomology* 29(4):582–98.
26. Mondet B, et al. (2005) Rainfall patterns and population dynamics of Aedes (Aedimorphus) vexans arabiensis, Patton 1905 (Diptera: Culicidae), a potential vector of Rift Valley Fever virus in Senegal. *Journal of Vector Ecology* 1905(June):102–106.
27. OIE Terrestrial Manual (2012) Aetiology Epidemiology Diagnosis Prevention and Control References. *Oie* pp. 1–5.